USDOT Region V Regional University Transportation Center Final Report

NEXTRANS Project No. USDOT-PU-4108-21574

A Multi-Scale Approach for Near-Surface Pavement Cracking and Failure Mechanisms

By

Hasan Ozer
Graduate Research Assistant
Civil and Environmental Engineering Department
University of Illinois at Urbana-Champaign
hozer2@illinois.edu

and

Carlos A. Duarte
Associate Professor
Civil and Environmental Engineering Department
University of Illinois at Urbana-Champaign
caduarte@illinois.edu

and

Imad L. Al-Qadi
Founder Professor of Engineering
Illinois Center for Transportation, Director
Civil and Environmental Engineering Department
University of Illinois at Urbana-Champaign
alqadi@illinois.edu

DISCLAIMER

Funding for this research was provided by the NEXTRANS Center, Purdue University under Grant No. DTRT07-G-005 of the U.S. Department of Transportation, Research and Innovative Technology Administration (RITA), University Transportation Centers Program. The contents of this report reflect the views of the authors, who are responsible for the facts and the accuracy of the information presented herein. This document is disseminated under the sponsorship of the Department of Transportation, University Transportation Centers Program, in the interest of information exchange. The U.S. Government assumes no liability for the contents or use thereof.

USDOT Region V Regional University Transportation Center Final Report

TECHNICAL SUMMARY

NEXTRANS Project No USDOT-PU-4108-21574 Final Report, 11.30.2010

Title

A multi-scale approach for near-surface pavement cracking and failure mechanisms

Introduction

Near-surface cracking is one of the predominant distress types in flexible pavements. The occurrence of near-surface cracking, also sometimes referred to as top-down cracking, has increased in recent years with the increased construction of relatively thick flexible pavements. However, understanding the mechanisms of near-surface cracking and its integration into pavement design protocols remains a challenge. A mechanistic-empirical approach requires a thorough understanding of the mechanisms of cracking on the surface or in the proximity of tires as well as an experimental characterization simulating field failure conditions. The analysis of this problem can become a very complex task due to multi-axial stress states in the vicinity of tires. This study investigated the near-surface response to non-uniform tire contact stresses and analyzed the potential for occurrence of cracks near the surface in a typical relatively thick flexible pavement structure. The Generalized Finite Element Method (GFEM) was utilized to analyze the pavement structures in three-dimensions (3-D) considering the viscoelastic effects. This method provided a computational framework where arbitrary orientation of cracks in a finite element mesh is possible. The use of the GFEM in this problem was particularly intended for resolving the mixed mode fracture conditions which may emanate from the complex stress states in the vicinity of tires.

Findings

A three dimensional (3-D) model for a typical pavement structure with a thick bituminous layer was built. The 3-D tire-pavement contact stresses were applied to the model. Cracks at aggregate scale were inserted at various locations and orientations within the pavement. The results from this numerical study showed that complex stress states in the presence of strong mode mixity may cause shear or tensile fracture in flexible pavements. Shear mode of fracture in the presence of compression (particularly in the proximity of tires) appears to be the dominant mode of damage. Tensile mode of fracture (also known as mode-I) clearly cannot describe the conditions near-surface in the proximity of tires. This study also highlighted the importance of novel computational methods, like the GFEM, on the discovery and understanding of mechanisms governing the premature failure of pavements.

Recommendations

In order to generalize the findings of this study, large pavement examples have to be extended to include wide-base tires, different pavement structures, and material properties. Simplified damage criteria based on one of the fracture parameters computed in the GFEM analysis should be identified as an index for near-surface cracking. This index can help in prediction of near-surface cracking in the field. The analysis was carried out using a static load. A moving load is important to simulate the effects of traffic loading.

Verification of the models used in this study is required. An experimental verification of the viscoelastic fracture model is necessary. Some field cracking data can be used to verify the predictions of the large scale pavement models.

Contacts

For more information:

C. Armando Duarte, Ph.D.
Associate Professor
Dept. Civil and Environmental Engin.
2122 Newmark Laboratory MC 250
University of Illinois at Urbana-Champaign
205 North Mathews Av.
Urbana, Illinois 61801 USA
Phone: (1)(217) 244-2830
Fax: (1)(217) 265-8040

NEXTRANS Center
Purdue University - Discovery Park
2700 Kent B-100
West Lafayette, IN 47906

nextrans@purdue.edu
(765) 496-9729
(765) 807-3123 Fax

www.purdue.edu/dp/nextrans

ACKNOWLEDGMENTS

The authors acknowledge the assistance and feedback from the members of the study advisory committee. The cost sharing provided by the Illinois Center for Transportation is greatly appreciated.

TABLE OF CONTENTS

Page

LIST OF FIGURES iv

CHAPTER 1. INTRODUCTION 1

1.1 Background and motivation 1

1.2 The Near-Surface Cracking Problem- A Literature Review 2

1.3 Study objectives 5

1.4 Organization of the research 6

CHAPTER 2. A BRIEF OVERVIEW OF THE GENERALIZED FINITE ELEMENT METHOD 8

2.1 Brief Background 8

2.2 GFEM- A Brief Overview 10

2.3 Enrichment Functions 13

CHAPTER 3. VISCOELASTIC CRACK ANALYSIS 17

3.1 Introduction 17

3.2 Schapery's Generalized *J*-integral 18

3.3 Numerical Examples 21

3.3.1 Edge-cracked bar 21

3.4 Summary and Remarks 26

CHAPTER 4. THE ANALYSIS OF NEAR-SURFACE CRACKING USING A THREE-DIMENSIONAL GFEM MODEL 28

4.1 Problem statement and Methodology 28
4.2 The Analysis of Near-Surface Cracking in Flexible Pavements 29
4.2.1 Three-Dimensional Pavement Model 29
4.2.2 Results from the Elastic Solution..... 33
4.2.3 Viscoelastic Crack Analysis 41
4.3 Summary and Remarks.....44

CHAPTER 5. CONCLUSIONS 46
5.1 Summary.....46
5.2 Future research directions.....47

REFERENCES 48

LIST OF FIGURES

Figure Page

Figure 2.1. A schematic of FE mesh with a discontinuity represented by (a) 9
Figure 2.2. One dimensional representation of partition of unity shape functions and various local approximations to a displacement field u(x). 12
Figure 2.3. Nodes affected by polynomial enrichments in a boundary value problem crossed by a crack. 14
Figure 2.4. Nodes affected by discontinuity enrichments in a boundary value problem crossed by a crack. 15
Figure 2.5. Nodes affected by near-tip enrichments in a boundary value problem crossed by a crack. 16
Figure 3.1. Crack front contours and failure assumption..... 19
Figure 3.2. Edge-crack bar geometry..... 23
Figure 3.3. The relaxation and compliance functions used in the numerical examples. .. 23
Figure 3.4. Edge-cracked bar example: (a) Undeformed configuration (b) Deformed configuration. 24
Figure 3.5. Comparison of J_v and W_f computed at the middle of crack front and at various 25
Figure 3.6. Crack opening near the crack tip at t = 15 *sec* as a function of temperature. . 26
Figure 4.1. Three dimensional pavement model with dual-tire contact stresses on the surface. Normalized transverse and vertical stresses are shown on each rib (contact stresses at each cell of the rib are normalized by the maximum vertical pressure). 30
Figure 4.2. The coordinates of surface and embedded cracks with respect to the dual-tire contact stresses on the pavement surface: (a) Top view of the pavement surface in the vicinity of dual-tire imprints; and (b) Coordinates of each crack on the surface and within the pavement. 31
Figure 4.3. Automatic crack front refinement illustrating locally graded meshes at the front domain of half-penny and circular crack. 33
Figure 4.4. Mohr-circle analysis of near-surface stresses under a dual-tire configuration. 34
Figure 4.5. Stress intensity factors (K_I and K_{II}) computed along the curved crack front (from θ=0° to 180°) of half-penny shaped cracks on the surface: (a) Cracks at 12.5 mm

away from the tire edge; (b) Cracks at 37.5 mm away from the tire edge; (c) Cracks at 62.5 mm away from the tire edge; and (d) Cracks at 87.5 mm away from the tire edge.. 36
Figure 4.6. Stress intensity factors (K_I and K_{II}) computed along the curved crack front (from θ=0° to 360°) of circular shaped cracks at 10 mm depth: (a) Cracks at 12.5 mm away from the tire edge; (b) Cracks at 37.5 mm away from the tire edge; (c) Cracks at 62.5 mm away from the tire edge; and (d) Cracks at 87.5 mm away from the tire edge.. 37
Figure 4.7. Stress intensity factors (K_I and K_{II}) computed along the curved crack front (from θ=0° to 360°) of circular shaped cracks at 20 mm depth: (a) Cracks at 12.5 mm away from the tire edge; (b) Cracks at 37.5 mm away from the tire edge; (c) Cracks at 62.5 mm away from the tire edge; and (d) Cracks at 87.5 mm away from the tire edge.. 39
Figure 4.8. Stress intensity factors (K_I and K_{II}) computed along the curved crack front (from θ=0° to 360°) of circular shaped cracks at 40 mm depth: (a) Cracks at 12.5 mm away from the tire edge; (b) Cracks at 37.5 mm away from the tire edge; (c) Cracks at 62.5 mm away from the tire edge; and (d) Cracks at 87.5 mm away from the tire edge.. 40
Figure 4.9. Stress intensity factors (K_I and K_{II}) computed along the curved crack front (from θ=0° to 360°) of circular shaped cracks at 60 mm depth: (a) Cracks at 12.5 mm away from the tire edge; (b) Cracks at 37.5 mm away from the tire edge; (c) Cracks at 62.5 mm away from the tire edge; and (d) Cracks at 87.5 mm away from the tire edge.. 41
Figure 4.10. Prony series representation of the relaxation and compliance functions. 42
Figure 4.11. The energy release rate computed at θ=90° along the circular crack at 60 mm depth and 60° plane to illustrate viscoelastic effects at −10°C and 21°C..... 44

CHAPTER 1. INTRODUCTION

1.1 Background and motivation

Accurately predicting performance and durability is essential to improving the design of new and existing pavements. Poor performance endangers public safety, increases maintenance costs, and furthermore causes unprecedented traffic congestion. The mechanistic-empirical design strategy has been proposed by Federal Highway Administration (FHWA) to design and construct more reliable pavements. The mechanistic-empirical approach provides realistic characterization of new and in-service pavements. The mechanistic component of the approach plays a critical role in characterizing and predicting the performance of pavements. Layered elastic theories and finite element method (FEM) are among the most known and popular mechanistic approaches. These techniques are often combined with continuum failure theories and empirical relationships to estimate flexible pavement failure mechanisms including fatigue, rutting, and thermal cracking.

Reliability and accuracy of the mechanistic methods are essential to understanding the mechanisms of failure in flexible pavements. Bottom-up fatigue, near-surface cracking (also known as top-down cracking), thermal cracking, and rutting are considered as major failure mechanisms. The methods utilized to tackle pavement failure include analytical and numerical methods. The FEM has become the most commonly used tool by many researchers to predict pavement response to vehicular and environmental response. However, two-dimensional (2-D) FEM, often used as the engine of the mechanistic methods, hinders proper characterization of pavement behavior under non-uniform tire pressures and environmental factors. This approach works to a certain

degree in the analysis of classical bottom-up fatigue cracking, where tensile stresses and strains govern the behavior at the bottom of pavement layers. On the other hand, FEM equipped with fracture and continuum mechanics tools poses a significant challenge to the analysis of the near-surface cracking problem, where crack initiation and propagation planes are not easily predictable.

Difficulties arise from the complex stress states generated by the tire-pavement contact stresses, strongly influential on or near the pavement surface. Three dimensional and non-uniform tire contact stresses in conjunction with the material inhomogeneity of the surface material renders the problem very difficult to analyze. Discrete element methods employing micromechanical theories can be useful; however, they are not yet computationally efficient in solving large scale problems. In addition, the acquisitions of continuum mechanics theories over the years and adaptability to FE type of methods are irrevocable. Therefore, FE based methods still remains a useful tool for continuum mechanics problems. Available methods surveyed in the literature do not provide an efficient and accurate way of predicting where and on which plane near-surface cracks originate and on which direction they will propagate.

1.2 Flexible Pavement Near-Surface Cracking

Near-surface cracking, also referred as top-down cracking, in flexible pavements is considered one of the predominant distress types affecting the ride quality as well as the structural integrity of pavements. As opposed to the classical fatigue cracking in relatively thin flexible pavements where cracks initiate from the bottom of bituminous layers, near-surface cracks initiate on or near the surface of flexible pavements. Near-surface cracking has become more common due to the increase in construction of long-lasting and relatively thick flexible pavements. For these types of pavement structures, cracking is usually confined to the surface layers. Heavy traffic and thermal loads are considered as the major source contributing to near-surface cracking in addition to stiffness gradients due to binder aging, variation in bituminous characteristics between lifts, and bituminous material segregation.

Many researchers have attempted to identify the causes and mechanisms of near-surface cracking. The majority of available literature on the subject focuses on field surveys and numerical studies. However, a few experimental studies have attempted to better understand the mechanisms of near-surface cracking. In one of these studies, full-scale and small-scale field experiments were designed to identify the influence of binder aging on top-down cracking in tropical climates (Rolt, 2000). The majority of cracks observed in the full-scale experiments were initiated from the surface layers of overlays. Another interesting observation from this study is that the cracks remained at a constant depth prior to propagating full depth. The hardening of asphalt binder with age was identified as the major contributor to cracking mechanism.

Uhlmeyer et al. (2000) conducted a comprehensive field survey in the state of Washington to seek traces of surface initiated cracks occurring especially in relatively thick flexible pavements. Surface initiated cracks were commonly observed in pavement layers typically exceeding 160 mm. Almost one third of the cores obtained from the field exhibited identifiable top-down cracks. Svasdisant et al. (2002) also conducted a field investigation to analyze the causes of surface initiated cracks in flexible and rubblized pavements. The authors utilized Falling Weight Deflectometer (FWD) tests and Indirect Tensile Strength (IDT) tests to validate their field observations. Field cores from eight sections exhibited surface cracks to various degrees. The authors attributed the mechanism of surface cracking primarily to tensile stresses that might develop outside the wheel path. According to the authors, thermal effects, binder aging, and construction-related problems also played an important role in aggravating the conditions.

Various laboratory tests were also performed to investigate surface initiated cracks. Wang et al. (2003) reported that near-surface cracking initiated at some distance from the surface in both tensile and shear modes when using a rolling wheel tests conducted at 60°C. Some cracks were observed along the plastic slip lines due to vertical loads applied on the surface. Similarly, De Freitas et al. (2005) conducted wheel-tracking experiments at high temperature to investigate near-surface cracking. The authors

identified shear stresses responsible for the initiation of the near-surface cracks. These cracks were also associated with the excessive permanent deformation under the wheel.

In addition to experiments and field surveys, various numerical methods have also been employed to better understand the mechanisms of near-surface cracking. Two-dimensional and three-dimensional FE models were utilized in conjunction with the linear elastic fracture mechanics theories. Kim et al. (2009) prepared a viscoelastic and axisymmetric FE model to investigate surface initiated cracks. A dissipated energy model was used to predict the extent of top-down cracking under repeated applications of loading at predefined locations. The extent of crack occurrence and damage was correlated to the amount of dissipated energy reaching a threshold. The dissipated energy ratio concept was also used by Wang et al. (2007). A mechanistic-empirical top-down cracking model was prepared to provide guidance for pavement engineers in Florida. According to the dissipated energy ratio concept, a strong correlation exists between the dissipated energy exceeding a certain threshold and crack occurrence. It has to be noted that layered elastic theories were used to compute stress and strain near the surface which was also used as an input to the dissipated energy computations.

A two-dimensional FE model of typical pavement structure coupled with linear elastic fracture mechanics was used to analyze near-surface cracks (Myers et al., 2000). Cracks at various positions with respect to the loading were inserted into the 2-D FE mesh. According to the FE results, it was concluded that surface-initiated crack propagation was primarily a tensile failure mechanism. Crack tip stress conditions resulted in the mode-I type of fracture. In another numerical study, De Freitas et al. (2005) used a 3-D FE model of wheel tracking tests and nonlinear viscoelastic material model to assess permanent deformations and potential cracking locations near the surface at relatively high temperatures.

The effects of dual and new generation wide base tire configuration on pavement cracking and particularly near surface failure were studied by Al-Qadi and his co-workers (Elseifi et al., 2005, 2006, Yoo and Al-Qadi, 2007, Al-Qadi et al., 2008, Wang and Al-Qadi, 2009). Realistic tire contact stresses were used in conjunction with a 3-D dynamic

model utilizing viscoelastic material characteristics. The analysis in these studies addressed the effects of shear stresses and their significant role on the initiation of surface cracks.

Analyzing near-surface cracking and understanding its real mechanisms pose significant challenges to researchers. The major challenges associated with the near-surface cracking problem in pavements can be summarized as follows:

- Tire-pavement contact stresses are generally non-uniform and can generate complex stress states;
- Complex stress states in the proximity of tires determines the conditions for both the onset of crack growth and the direction of crack propagation;
- Stiffness gradients within the pavement in addition to potential inhomogeneities due to construction related problems can aggravate conditions for cracking.

In order to accurately identify the damage mechanisms of near-surface cracking considering the factors listed above, a method that can predict crack initiation and growth in arbitrary orientations is needed. It is very likely that crack front conditions determined by multi-axial stress state may induce mixed mode of cracking. Therefore, pure tensile failure theory usually employed for the bottom-up fatigue cracking considering only mode-I cracking ignores the failure potential in other modes of cracking and 3-D effects at the crack front. Multi-axial stresses in the proximity of tires also renders the near-surface cracking problem troublesome since the orientation for the onset of crack growth and direction of crack propagation can not be known a-priori.

1.3 Study objectives

The objective of this study is to analyze near-surface cracking in flexible pavements due to non-uniform tire-pavement interactions. A novel numerical technique was used as a means to identify the extent of traffic loads on pavement cracking in the proximity of tires. Three-dimensional and highly multi-axial nature of the problem was

captured by this method, which was ideally designed for 3-D fracture problems for complex geometries and mixed loading conditions.

1.4 Organization of the research

In order to achieve the objectives of this study, the following strategy was followed. The methodology proposed is composed of three major tasks described in the following:

- A three-dimensional viscoelastic constitutive model was implemented in order to characterize the response of the bituminous layers in the pavements. The viscoelastic algorithm compatible with those implemented in the commercial FE packages was implemented in the Generalized Finite Element Method (GFEM). The GFEM was chosen as the numerical tool to tackle the problem of this study. The GFEM and/or the Extended Finite Element Method (XFEM) are two novel techniques for problems with complex geometry, loading conditions, and also multi-scale applications. They are promising candidates to overcome mesh design and computational issues of the standard FE methods for the problems with discontinuities such as cracks, material interfaces etc. This task involved code implementation and verification examples to test the robustness and accuracy of the implementation.
- The implementation of the domain integral formulations to compute viscoelastic crack front parameters such as time/temperature dependent energy release rate or work of fracture in the GFEM constituted the second major task of this study. Viscoelastic fracture analysis was done using the *J*-integral method and domain integral formulations. The *J*-integral within a domain integral framework was chosen to investigate the contribution of viscoelasticity to the onset of crack growth. This approach was proven to be a computationally efficient way of computing fatigue crack growth for elastic as well as inelastic materials. A domain integral implementation similar to that of standard FE method was integrated to the GFEM framework. A viscoelastic fracture model available in the literature was extended to

domain integral formulations. Similar to the first task, this task also involved code implementation and verification examples in addition to the mathematical formulations for the domain integral approach.

- The GFEM, equipped with the tools proposed in the aforementioned tasks, provides a computationally efficient platform to analyze cracking flexible pavement structures. A three-dimensional model of typical pavement structures was prepared to analyze near-surface cracking.

1.5 Outline of the Report

The outline of this report is as follows. First, the near-surface cracking problem is presented along with the literature findings to characterize this problem experimentally and numerically. A brief introduction to the GFEM is presented in the next section to highlight some of the most important features of the method. This chapter also presents historical development of the method. Viscoelastic material and fracture model implemented in the GFEM is described in Chapter 3. This chapter presents the numerical algorithm as implemented in the nonlinear solver of the GFEM along with some verification examples. Chapter 4 presents the solution of a large scale pavement problem with a typical thick flexible pavement structure. This example is aimed at finding the critical location and orientation for near-surface crack initiation.

CHAPTER 2. A BRIEF OVERVIEW OF THE GENERALIZED FINITE ELEMENT METHOD

This chapter presents a brief background on an alternative approach recently emerged as a viable technique in the solution of fracture and delamination problems. Basic constitutive relationships and fundamental theoretical aspects of the method along with the historical background are introduced. Some of the other available methods used in fracture and delamination problems are also introduced within the literature review and background information.

2.1 Brief Background

Interface elements within the framework of the FEM have been commonly used in modeling geometrical discontinuities that can exist in a variety of structures such as pavements, foundations, and buildings. Interface elements were incorporated into the FE computations to capture displacement jumps at the discontinuities. Interface elements have first been introduced by Mahtab and Goodman (1970) and Zienkiewicz et al. (1970) to describe load transfer in rock joints with a linear Mohr-Coulomb friction model and plasticity. Later, similar interface elements and models were incorporated in the FEM for the numerical treatment of soil-structure interactions (Desai et al., 1984, 1985), delamination in composite structures (Chaboche et al., 1997a,b, Alfano and Crisfield, 2001, 2003, Alfano and Sacco, 2006), and fracture in quasi-brittle materials (Stankowski and Runesson, 1993, Carol et al., 2001). The interface element technology is usually coupled with cohesive zone models (Xu and Needleman, 1994, Ortiz and Pandolfi, 1999) to model crack growth in fracture problems.

Displacement jumps due to geometrical or material discontinuities are often described by the relative displacements of a set of double nodes inserted in a FE mesh. The double node set constitutes zero-thickness interface elements. In the solution of fracture and delamination problems, these elements have to be inserted at interelement boundaries. Interface elements have their own compliance (usually referred as artificial compliance), which in turn alter the stiffness of the bulk structure. In order to use cohesive elements, a-priori information for the crack propagation path is needed. This information is usually available for the delamination problems where the interface in a composite structure is known. However, crack propagation path is not always available for problems with complex geometries and loading conditions. In this case, cohesive zone elements are usually inserted along a large number of element boundaries, which can alter the compliance of the structure significantly. For example, cohesive element approach is certainly prohibitive for the analysis of near-surface cracking due to unpredictable nature of crack initiation and propagation. In addition to the artificial compliance problem of the interface elements, mesh design is also very labor intensive task especially for 3-D fracture problems.

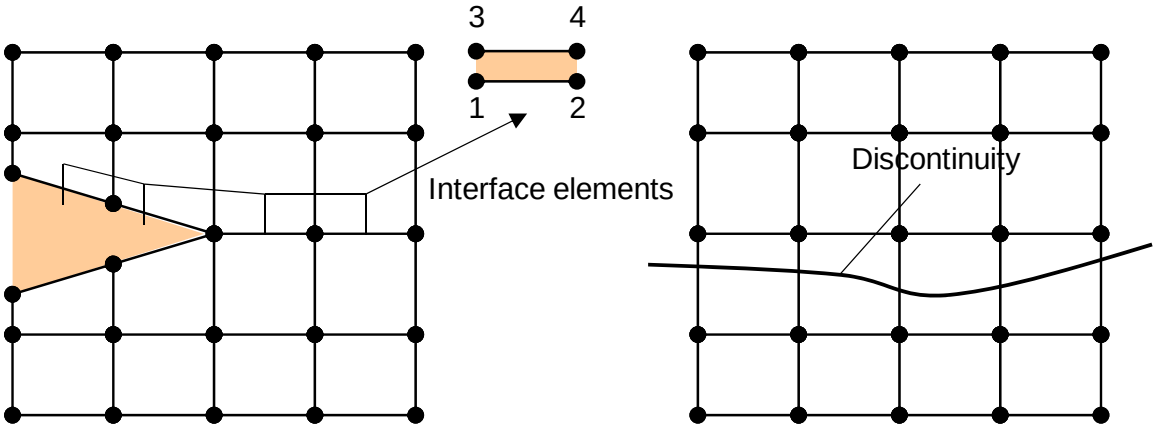

Figure 2.1. A schematic of FE mesh with a discontinuity represented by (a) Interface elements (b) discontinuity enrichments

An alternative approach employs the partition of unity property of FE shape functions to represent discontinuities. The Generalized Finite Element Method (GFEM)

and the Extended Finite Element Method (XFEM) are promising candidates to overcome mesh design and computational issues of the standard FEM for the problems with discontinuities such as cracks, material interfaces etc. Within this approach, the standard approximation functions are enriched locally with special functions, also referred as enrichment functions, representing the local behavior of the solution. The key difference between standard finite elements and GFEM/XFEM type of methods is the possibility of arbitrarily locating the discontinuity within the domain of the problem. This difference is illustrated in a schematic shown in Figure 2.1.

The GFEM/XFEM type of methods brings great freedom for the selection of customized enrichment functions representing various local features. The customized enrichment functions can be used to model cracks (Dolbow et al., 2000, Duarte et al., 2001, Moes et al., 2002, Oden and Duarte, 1997, Sukumar et al., 2000) and edge singularities (Duarte et al., 2000). In addition, the theory and the data structure behind the XFEM/GFEM also lend itself naturally to multiscale applications since local approximations can be used to enhance the solution at the global scale. Some of the examples of customized enrichment functions to bridge the scale between local and global scale are used to model voids, inclusions (Sukumar et al., 2001, Strouboulis et al., 2004), and microstructure (Sukumar et al., 2003, Simone et al., 2006). The GFEM has recently been extended to a global-local approach (Kim et al., 2008, 2009a), where the global problem uses local solutions as customized enrichment functions.

2.2 GFEM- A Brief Overview

The objective of this section is to illustrate the highlights and major features of the GFEM employed in the analysis of the near-surface cracking problem in pavements. The GFEM that evolved in the works of Duarte et al. (1996, 1997, and 2000) and Strouboulis (2004) is a special case of the so-called partition of unity based methods. The GFEM differs from the standard finite element by the trial functions used to approximate displacement fields. For example, a partition of unity based approximation of a scalar

displacement field $u_h(\mathbf{x})$ can be expressed with partition of unity shape functions and nodal coefficients

$$u_h(\mathbf{x}) = \sum_{1}^{N} \varphi_\alpha(\mathbf{x}) u_{h\alpha}(\mathbf{x}) \tag{1}$$

where φ_α constitute partition of unity ($\sum_{\alpha=1}^{N} \varphi_\alpha(\mathbf{x}) = 1$) for all x in the domain of discretization, α is a node in FE discretization, and $u_{h\alpha}(\mathbf{x})$ are nodal coefficients representing local approximations. The most commonly used partition of unity functions are from the Lagrangian family of functions, which also forms the basis of the standard FE method.

The GFEM differs from the FEM in the description of the local approximations defined in Equation 1. The nodal coefficients, $u_{h\alpha}(\mathbf{x})$, are the nodal displacements or rotations in the standard FEM whereas the GFEM adds another layer of approximation in the local level to compute these nodal coefficients. This feature is commonly referred to as the enrichment functions in the GFEM. Equation 2 describes the use of the enrichment functions for the local approximations.

$$u_{h\alpha}(\mathbf{x}) = \sum_{i=1}^{D_L} a_{i\alpha} L_{i\alpha}(\mathbf{x}) \tag{2}$$

where $a_{i\alpha}$ are nodal coefficients, $L_{i\alpha}$ are enrichment functions, $i = 1, \ldots, D_L$. The local approximation function, $u_{h\alpha}(\mathbf{x})$, is a local approximation of the field $u(\mathbf{x})$ defined as the support of the partition of unity function φ_α. The support of a node α, w_α, denotes a subdomain of the FE discretization where the partition of unity function is nonzero. This concept is illustrated in Figure 2.2 with a one-dimensional (1-D) schematic. The displacement field that needs to be approximated using the GFEM approximation functions might have strong gradients, kinks, or jumps. All of these features might have a physical correspondence, and they might only exist locally, as shown in the conceptual

schematic. For example, displacement jumps may correspond to displacement differences across a crack face. Kinks might represent changes in the displacement due to material interfaces. On the other hand, strong gradients are the implications of crack tip behavior where displacements exhibit an asymptotic behavior.

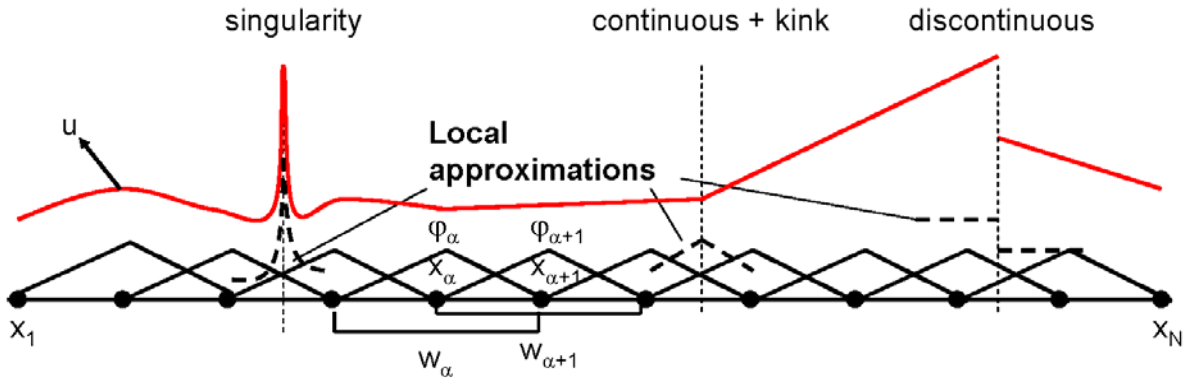

Figure 2.2. One dimensional representation of partition of unity shape functions and various local approximations to a displacement field u(x).

Several methods can be used to approximate the type of local features as shown in Figure 2.2. The FE method utilizes piecewise smooth functions (hat-like functions as shown in Figure 2.2) to approximate the displacement field. In this case, the only way to represent such local features is to match element boundaries with the local feature such as a material interface or a crack. This is usually done in nicely structured meshes around the interface or crack with very small elements in the vicinity of these local features. On the other hand, the GFEM offers an alternative approach in the form of an enrichment strategy using such functions in Equation 2 to enhance the solution in the vicinity of the local features. This approach eliminates the difficulties associated with mesh design using unstructured meshes that are not necessarily matching element boundaries. In this case, local enrichment functions are used to enhance the accuracy of approximation. The details of the theoretical aspects of the GFEM can be found elsewhere (Duarte and Oden 1996a,b, Duarte et. al. 2000 and 2001). This approach has recently been used to solve fracture problems in complex geometries where mesh design is particularly a challenging task as well as problems that require high accuracy in the computation of crack front

parameters (Duarte et. al. 2000 and 2001, Sukumar et. al. 2000 and 2001, Moes et. al. 2002, Pereira et. al. 2009a,b).

In this study, the implementation of the GFEM presented by Pereira et al. (2009a,b) is used to analyze the near-surface cracking problem. The enrichment strategy employed includes polynomial enrichment functions, step functions, and asymptotic enrichment functions. The polynomial enrichment functions are used to increase the order of approximation of a whole domain or a specified subdomain. The step functions describe displacement jumps across crack faces whereas asymptotic expansion of the elasticity solution is used near the crack fronts to represent singular crack tip behavior. This enrichment strategy can also be extended to linear viscoelasticity since crack tip singularity can be assumed to be preserved for linear viscoelastic problems and for small deformations.

2.3 Enrichment Functions

The selection of enrichment functions for a particular local space depends on the displacement field over this local domain. Strong displacement gradients, discontinuities, and crack tip singular fields that would otherwise be poorly approximated by smooth functions can be represented by these local enrichment functions to improve accuracy of approximation of the global displacement field u(x). This displacement field can be decomposed into components to represent local and global behavior independently. Global behavior can be represented by a continuous function. On the other hand, specifically for fracture problems, local displacement field are composed of two separate local fields representing crack tip singularity and discontinuity due to crack surfaces. Therefore, one can select approximation functions based on a priori knowledge of the displacement field and the crack surface geometry. The GFEM can utilize singular type of crack tip solution as enrichment functions at the crack front and step functions to discretize crack surfaces. High-order polynomials can also be used as continuous enrichment functions to improve the accuracy of continuous part of the displacement

field. Readers are referred to (Duarte et al., 2000, 2007, Pereira et al., 2009a,b) for details of special enrichment functions and details of enrichment strategy used in the GFEM.

Three major enrichment functions were used in this study. First are the polynomial enrichments for increasing the order of approximation. A smaller domain of interest can also be chosen to apply enrichments as illustrated by the schematic in Figure 2.3. This will result in high-order approximation of the displacement field u at the nodal supports of enriched nodes only. In contrast, such high-order approximations can be considered analogous to the high-order elements in standard finite element method (e.g. 10-node tetrahedral, 27-node hexahedral etc.) without any changes in the element node numbering. High-order approximation in the GFEM can be achieved by adding enrichments to the parent element (i.e. a 4-node tetrahedral or 8-node hexahedral) hierarchically.

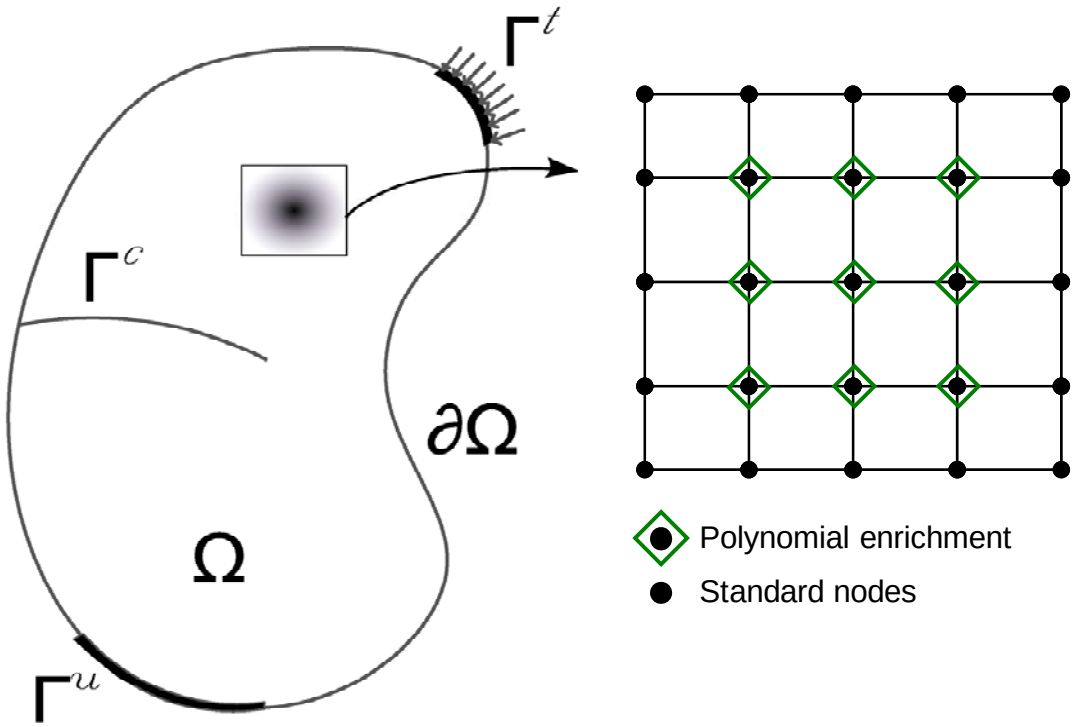

Figure 2.3. Nodes affected by polynomial enrichments in a boundary value problem crossed by a crack.

Second types of enrichments are discontinuity enrichments. Discontinuity enrichments are provided by step functions imposed on the nodes of elements cut by crack. Figure 2.4 illustrates the set of nodes affected by discontinuity enrichments.

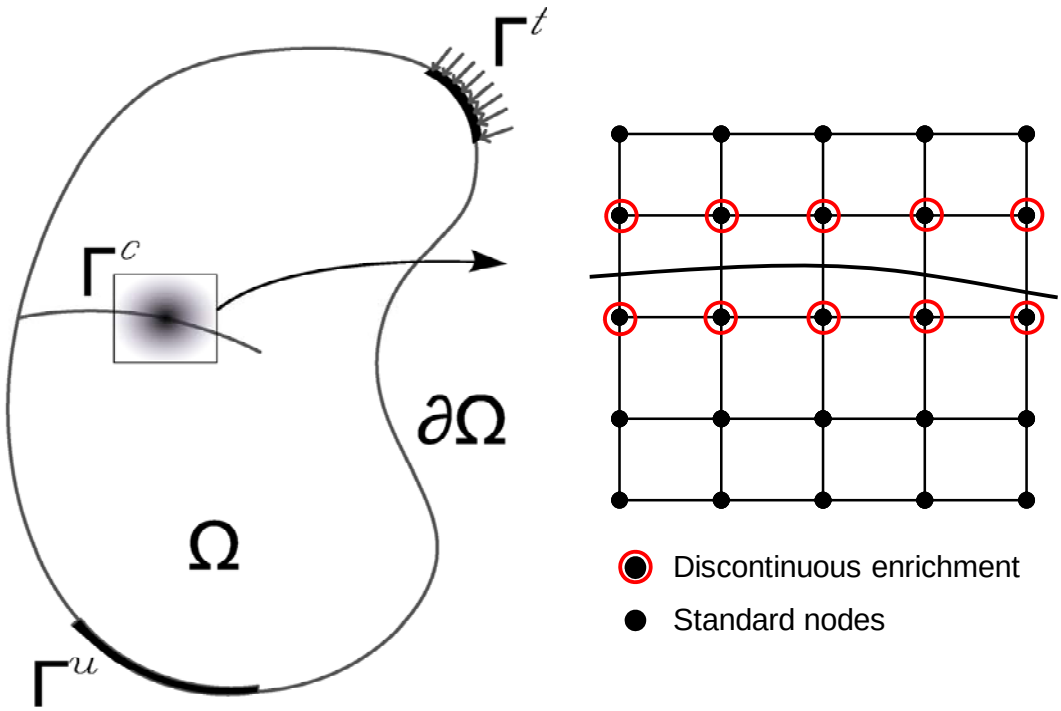

Figure 2.4. Nodes affected by discontinuity enrichments in a boundary value problem crossed by a crack.

Third types of enrichments are near-tip enrichments. This type of enrichment functions are obtained from the asymptotic expansion of the elasticity solution. They are imposed near the crack fronts to represent singular crack tip behavior. Figure 2.5 illustrates the nodes affected by the near-tip enrichments.

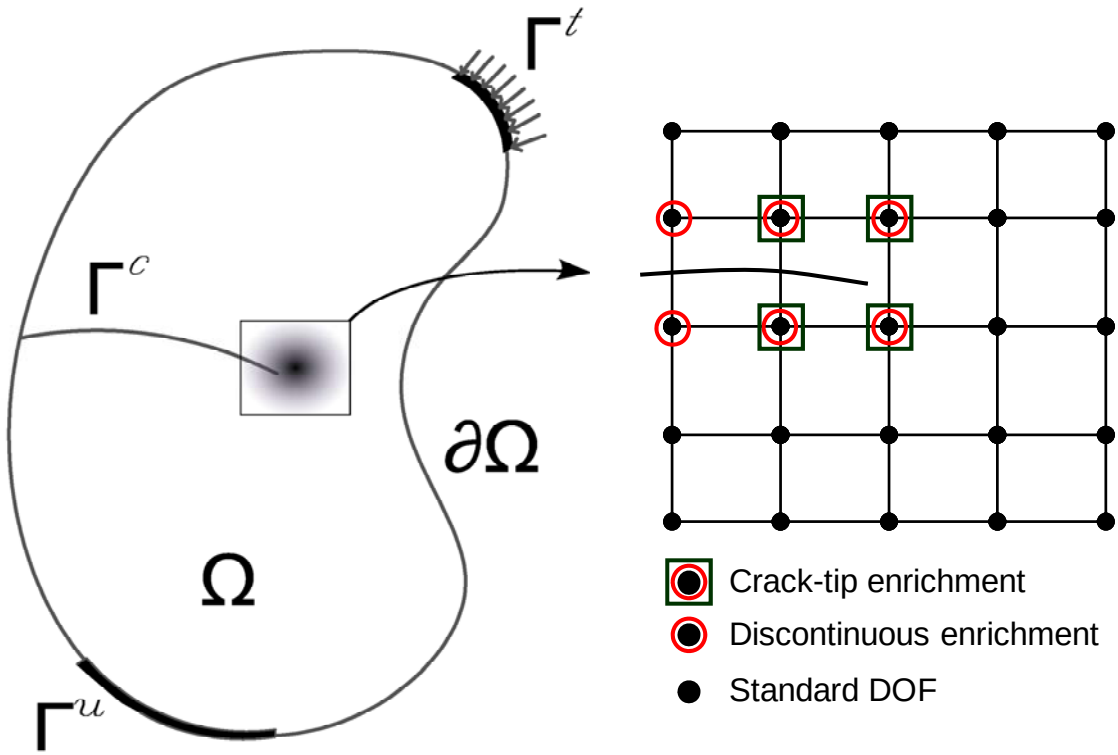

Figure 2.5. Nodes affected by near-tip enrichments in a boundary value problem crossed by a crack.

CHAPTER 3. VISCOELASTIC CRACK ANALYSIS

Chapter 3 presents a brief overview of the viscoelastic crack analysis implemented in this study. This chapter discusses the Schapery's generalized *J*-integral approach as well as domain integral conversion of Schapery's contour *J*-integral. The extension of Schapery's viscoelastic fracture model to the domain integral form is presented. Several numerical examples were solved to verify accuracy of the proposed approach as well as illustrate time and temperature dependence of the fracture parameters.

3.1 Introduction

The present chapter describes the implementation of a computationally efficient viscoelastic crack analysis tool within the Generalized Finite Element Method (GFEM). The proposed approach benefits from a very useful numerical tool (GFEM) used for fracture problems in complex 3-D structures. The implementation of viscoelastic fracture model contains two major tasks. First is the implementation of a linear viscoelastic material model using a nonlinear Newton-Raphson scheme within the GFEM. Generalized Maxwell Model (GMM) is used as a mechanical analog to represent linear viscoelastic behavior in the bulk material. It is known that Poisson's ratio for viscoelastic can also be time dependent. The approach implemented has the flexibility to evaluate materials with varying Poisson's ratio. Second major task of the implementation presented herein is the extension of Schapery's generalized *J*-integral (Schapery, 1984, 1990) to a domain integral form introduced by Shih et al. (1986) and Moran and Shih (1987). Domain integral allows for the computation of energy release rate and it is ideally suited for 3-D fracture problems.

3.2 Schapery's Generalized J-integral

The *J*-integral theory has been applied to elastic and time-independent inelastic materials successfully (Rice, 1968). However, methods for characterizing and predicting crack growth for time-dependent inelastic materials are significantly limited. Most of the work done for fracture in time-dependent materials is limited to failure characterization at varying temperatures and crack speed and analytical formulations employing classical singular crack tip functions. The major difficulty associated with defining fracture parameters in viscoelastic materials is related to the very definition of energy release rate and energy balance. Fracture energy represents how much energy is physically dissipated during the physical processes of fracturing. However, viscoelastic materials can also dissipate energy through viscous deformations in the bulk of the structure. Since viscous deformations are not limited only to the crack front, farfield contours selected to compute *J*-integral can not be used for computing available energy for crack growth. However, the generalized *J*-integral approach (Schapery, 1984 and 1990) utilizes correspondence principle, which makes use of elastic solution and well established theories for elastic materials. The main premise of this integral form is the elimination of time-dependent variables from the integral equation to compute the *J*-integral in a corresponding reference elastic state. This form is identically equal to the Rice's *J*-integral and preserves all of the essential properties, such as the path independency. The approach is also compatible with finite element implementation. The generalized *J*-integral approach for linear viscoelastic materials is reviewed in this section and GFEM implementation details is also discussed very briefly.

Schapery (1984) defined a path independent integral, J_v, representing mechanical crack tip energy derived from a reference elastic solution of a viscoelastic problem. This form derives from the correspondence principle referring to the elastic-viscoelastic relationships and pseudo variables. It allows construction of viscoelastic solution from a reference elastic solution. The terms in J_v integral are from the reference elastic solution, which preserves path independence of the J_v -integral.

$$J_v = \int_{C_1} W^R dx_2 - T_i \frac{\partial u_i^R}{\partial x_1} ds \tag{1}$$

where T is the traction vector defined on the contour C_1, W^R is pseudo strain energy density, and u_i^R is pseudo displacement. This form proposed by Schapery (1990) is a contour integral mainly used to characterize fracture in 2-D problems as shown in Figure 3.1. The path C_1 for J_v is arbitrary and it starts and ends on the unloaded faces of the crack. This allows the use of farfield solution to compute crack driving force. However, as discussed in details in the preceding chapter, domain integral methods are preferable for 3-D characterization of a crack fronts. Therefore Schapery's generalized *J*-integral was extended to domain integral formulations. We recall the domain integral derived for elastic materials (Moran and Shih, 1986).

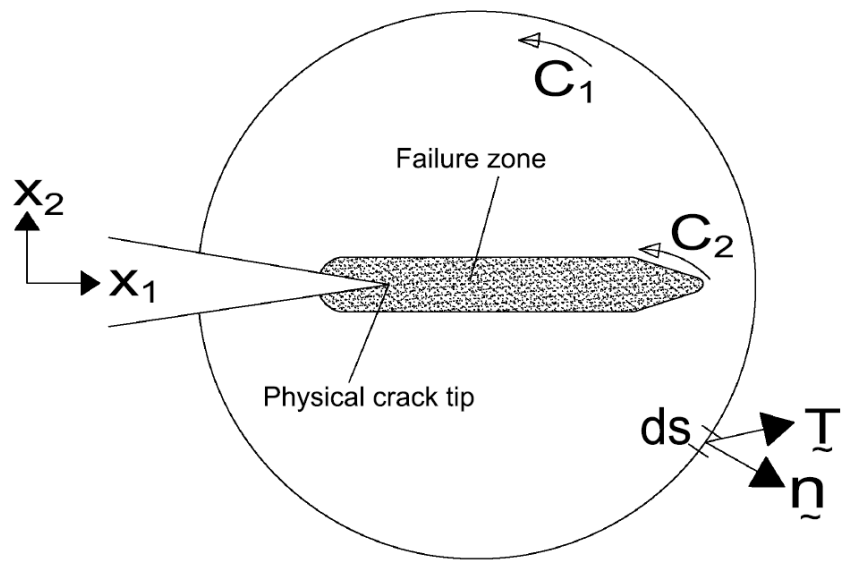

Figure 3.1. Crack front contours and failure assumption.

$$J(s) = \frac{-\int_V (Wq_{k,k} - \sigma_{ij} u_{i,k} q_{k,j}) dV}{\int_\Gamma w(s) ds} \tag{2}$$

where V is the volume enclosing the crack front in the vicinity of point s, W is the strain energy density, $\boldsymbol{\sigma}$ is stress tensor, $\mathbf{u}$ is displacement vector, $\mathbf{q}$ is auxiliary weight function defined in V whose value is 1 at the crack front, 0 at the boundaries of V, and arbitrary (between 0 and 1) elsewhere, and finally $w(s)$ is the values of $\mathbf{q}$ computed at the crack front Γ. Also note that subindices following the comma denote gradients such as $u_{i,k} = \dfrac{\partial u_i}{\partial x_k}$.

The J-integral given by Equation (2) can be extended for viscoelasticity problems using Schapery's correspondence principles and fracture model. The path-independent J-integral for viscoelastic materials can be converted to a domain integral by replacing the solution variables with their counterparts from the reference elastic solution, also known as pseudo-variables. The details of pseudo-variables concept for viscoelastic constitutive equation can be found in the works of Schapery (1984 and 1990). The J-integral for a reference elastic solution, also known as the generalized J-integral, can then be defined in the following form:

$$J_v(s) = \frac{-\int_V (W^R q_{k,k} - \sigma_{ij} u^R_{i,k} q_{k,j}) dV}{\int_\Gamma w(s) ds} \tag{3}$$

where W^R is the pseudo strain energy density and $\mathbf{u}^R$ is pseudo-displacements. The relationship between pseudo and real variables is given as follows

$$\begin{aligned} f^R &= \frac{1}{E^R} \int_0^t E(t-\tau) \frac{\partial f}{\partial \tau} d\tau \\ f &= E^R \int_0^t D(t-\tau) \frac{\partial f^R}{\partial \tau} d\tau \end{aligned} \tag{4}$$

where E^R is the reference modulus (taken as instantaneous modulus in this study), $E(t)$ is the relaxation function, and $D(t)$ is the compliance function.

The generalized *J*-integral is a domain independent crack front parameter deduced from the far-field stresses and displacement fields of a reference elastic solution. This parameter merely represents the crack front fields for a reference elastic solution and does not reflect the time-dependent nature of the crack tip response. To address the viscoelastic crack front response, Schapery (1984) defined a total mechanical work input (or work of fracture) to the crack front in terms of the generalized *J*-integral (J_v). Using this form results in the energy release rate (or J_v) using the well established path or domain integrals and far-field solution of the problem. In addition, it can be redefined to describe time and temperature dependent crack front states:

$$W_f = E^R \int_0^t D(t-\tau) \frac{\partial J_v}{\partial \tau} d\tau \tag{5}$$

3.3 Numerical Examples

In this section, several numerical examples to test the implementation of viscoelastic crack analysis are presented. The same problems were solved with commercial software (Abaqus) for comparison. Another objective of the tests examples is to illustrate the effect of time and temperature influence at the onset of crack propagation using the proposed viscoelastic crack model in the GFEM.

3.3.1 **Edge-cracked bar**

A brief introduction to the GFEM procedure for solving fracture problems is briefly revisited. Locally refined meshes with increasing degree of polynomials were used in the GFEM to tackle fracture problems. Crack surfaces were introduced to the model as a separate entity. Step functions and crack tip singular functions were used as enrichments to describe crack surface and approximate singular displacement fields at the crack front, respectively. In addition, regular polynomial enrichments were also used to increase the accuracy of approximation. The whole procedure, including crack surface detection, refinement and/or unrefinement, enrichment, and solution has been implemented in an automated procedure. Details of this analysis approach can be found elsewhere (Duarte et al., 2007, Pereira et al., 2009a,b). This integrated approach was now

extended to viscoelastic materials and crack initiation in this study. A brief summary of this integrated approach is described in the following:

1. Pre-processing to generate a coarse mesh for the problem domain and prepare a mesh to discretize crack surface
2. Detection of crack surface and front
3. Refinement of crack fronts to create a locally refined mesh
4. Assignment of enrichment functions to the selected nodes
5. GFEM solution of the problem (using nonlinear solver for inelastic materials)
6. Post-processing the results to compute energy release rate or SIF's along the crack front

Edge-cracked bar is a very commonly used example in the development and verification of new numerical and mathematical strategies to compute energy release rate and/or SIF's (Li et al., 1998, Pereira et al., 2009a). The solution of the same problem using domain integral method and linear elastic material properties was presented in the previous chapter. Edge-crack example was extended to viscoelasticity and viscoelastic crack model whose details were described in this chapter.

The problem consists of a rectangular bar sliced by a through the thickness crack as shown Figure 3.2. The geometry was taken as h/t = 0.875, a/t = 0.5, and w/t = 1.5. As for the material properties, linear viscoelastic model was used. Crack front elements were locally refined to the levels of Le/a ratios around 0.069. Figure 3.3 illustrates the master curves plotted using the Prony series coefficients of the relaxation and compliance functions. Instantaneous Poisson's ratio was set to 0.3.

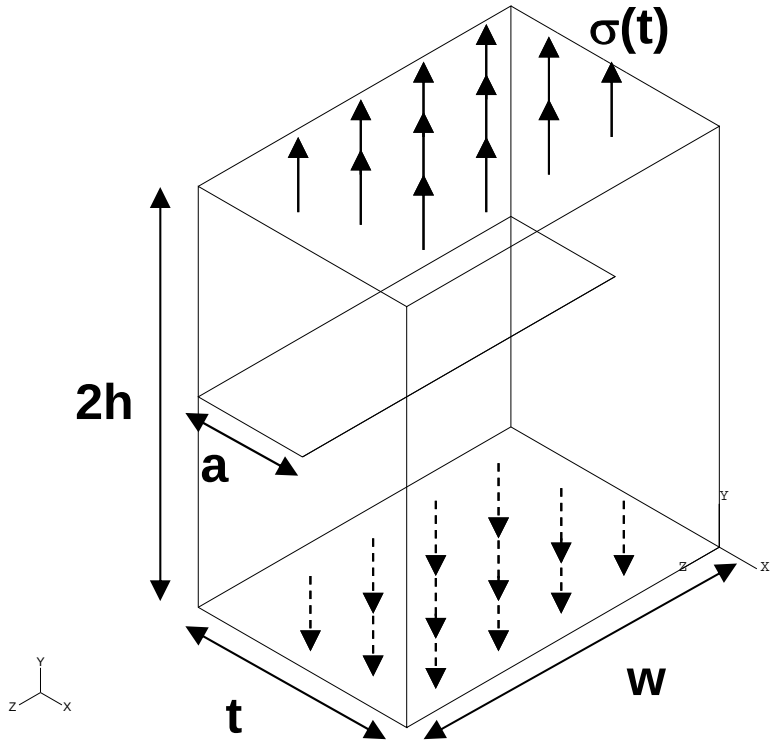

Figure 3.2. Edge-crack bar geometry.

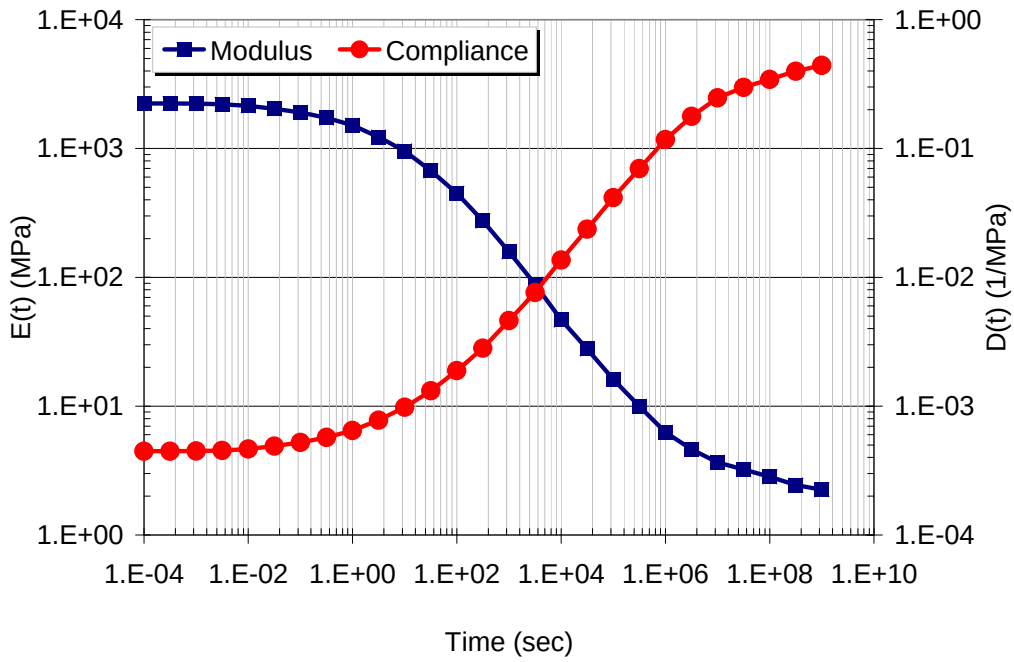

Figure 3.3. The relaxation and compliance functions used in the numerical examples.

Figure 3.4 illustrates undeformed and deformed configuration of the solution after automatic crack front refinement. The elements at the crack front and across the crack surface are divided into integration elements for integration purposes.

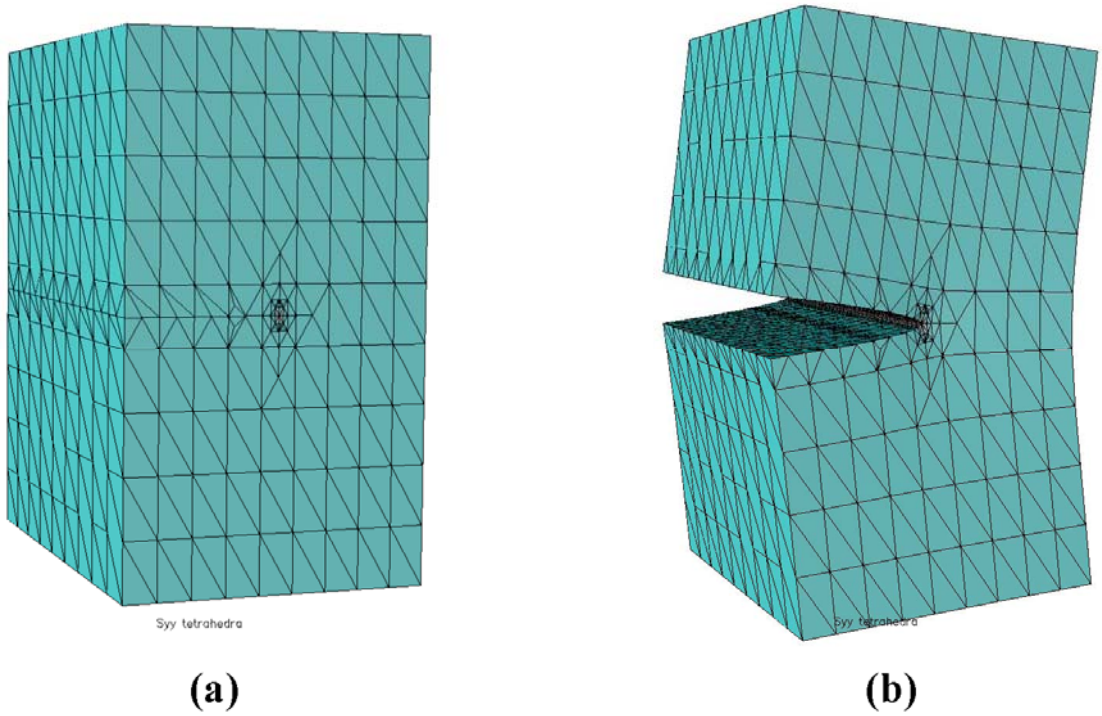

Figure 3.4. Edge-cracked bar example: (a) Undeformed configuration (b) Deformed configuration.

Using the solution variables at the crack front and Equation 3 and 5, crack front parameters can be computed. Figure 3.5 shows a comparison between Schapery's J_v-integral and work of fracture W_f computed in the middle of crack front. Applied load in this example is also shown as an insert to this figure. One of the major objectives of this exercise is to show how temperature and time influence the mechanical work available for crack growth. As temperature increases, the effects of creep become more pronounced and increases work of fracture. On the other hand, J_v-integral remains insensitive to temperature variations. This is expected because J_v-integral was computed at a reference elastic solution, which is not rate and temperature dependent. This type of rate-temperature dependency is also consistent with the findings of other viscoelastic crack

models (Masuero and Creus, 1993, 1995, Moutou Pitti et al., 2009, Pitti et al., 2007, Soon Lee and Jong Kim, 1995, Suo et al., 2003). The importance of this observation was materialized when time to crack initiation needs to be predicted under various loading conditions. Given the fracture energy of a material (G_c) at a specific temperature, one can calculate the crack initiation time (time when the work of fracture becomes equal or greater than the fracture energy of the material).

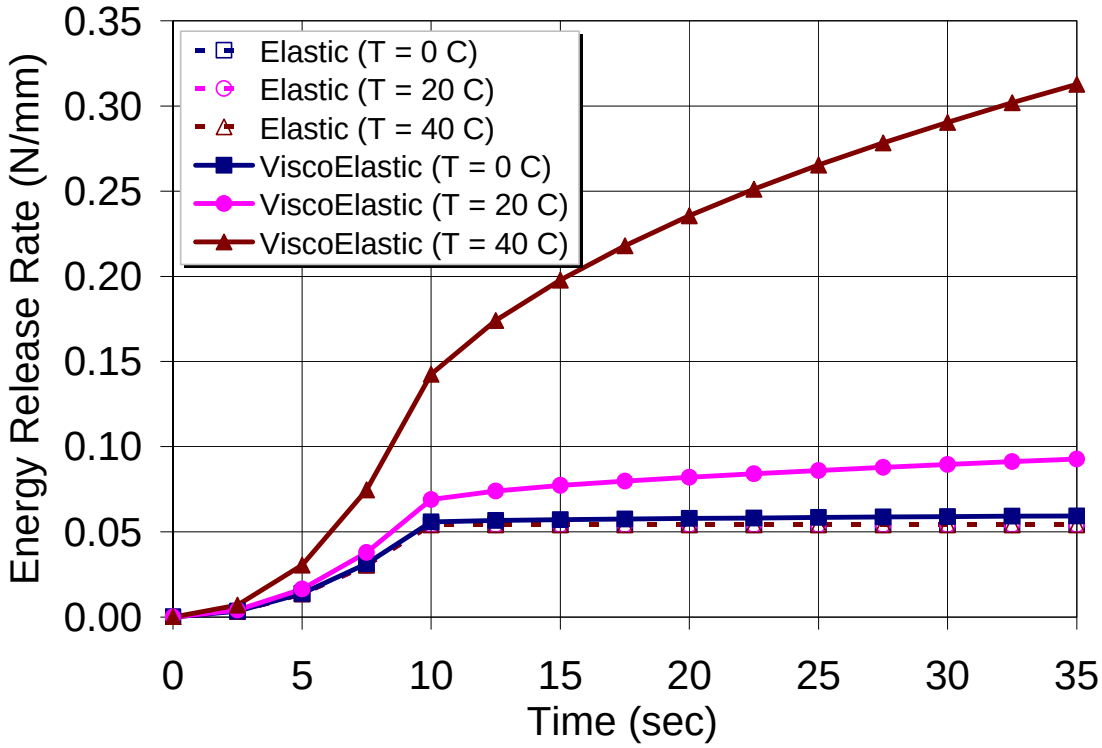

Figure 3.5. Comparison of J_v and W_f computed at the middle of crack front and at various temperatures under ramp and creep load.

Another example with the edge-crack is to demonstrate crack opening with temperature variations. The effect of creep on crack opening at different temperatures is illustrated in Figure 3.6. This figure shows the shape of the crack at t = 15 sec and at the same applied external load. The shape of the crack obtained from the elastic solution is also added to the figure. It is clearly seen that the crack becomes increasingly blunt and it has a curvature several orders of greater than that of elastic crack as temperature

increases.. This observation is consistent with the literature findings (Mueller, 1971, Knauss, 1989).

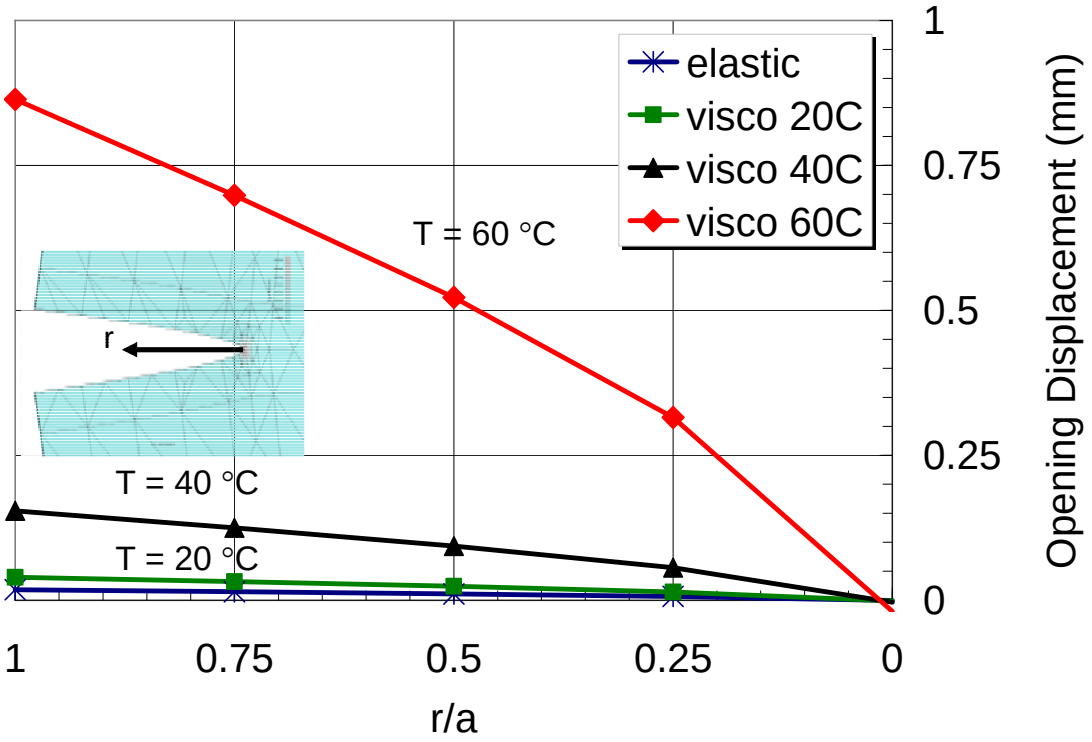

Figure 3.6. Crack opening near the crack tip at t = 15 *sec* as a function of temperature.

3.4 Summary and Remarks

In this chapter, basic constitutive relationships of a viscoelastic fracture model were reviewed. Viscoelastic constitutive relationships and an algorithm to implement viscoelasticity in the GFEM were described in details. The procedure employed is based on finding the algorithmically consistent tangent stiffness. This ensures convergence in one iteration. Implementation was tested with simple verification examples. Secondly, a viscoelastic fracture model introduced by Schapery (1984, 1990) was revisited. The fracture model originally proposed by Schapery for viscoelastic materials is based on a generalized *J*-integral computed as a contour integral. The extension of the generalized *J*-integral to domain integral is necessary for 3-D fracture problems. The generalized *J*-

integral originally proposed as a contour integral was extended to the domain integral version as described in the previous chapter. Implementation of domain integral version of the Schapery's *J*-integral in the GFEM was also described herein. Similar to the viscoelasticity implementation, an incremental procedure is followed with the use of information only from the previous solution step.

The generalized *J*-integral preserves path independency of the *J*-integral which can be a critical issue for materials dissipating energy due to creep. Therefore the use of farfield solution is enabled with the generalized *J*-integral which merely yields the energy release rate for a reference elastic solution of a viscoelastic problem. This integral was then converted to time domain using a convolution integral to consider time and temperature effects. Time and temperature effects were reflected to this relationship using shift functions obtained from modulus testing.

Several benchmark fracture problems were solved to demonstrate the key features of the implementation. The influence of time and temperature on the energy release rate or work of fracture was illustrated. Creep effects become increasingly influential as the temperature increases above 0°C for the examples shown in this chapter.

CHAPTER 4. THE ANALYSIS OF NEAR-SURFACE CRACKING USING A THREE-DIMENSIONAL GFEM MODEL

This chapter introduces a novel numerical approach for the analysis of near-surface cracking in flexible pavements. Section 4.1 describes the near-surface cracking problem and discusses the issues with the analysis of the problem. Section 4.2 presents the three dimensional pavement model for the analysis of near-surface cracking in thick flexible pavements. Three-dimensional pavement model with cracks inserted at various locations is also introduced. Section 4.3 discusses the results and discussions from the numerical analysis with cracks at various locations. Finally, Section 4.4 presents the extension of the analysis approach to viscoelasticity and viscoelastic fracture mechanics.

4.1 Problem statement and Methodology

The mechanistic analysis of near-surface cracking poses significant challenges particularly due to high and non-uniform tire contact stresses. Tires generate complex stresses within the pavement in the vicinity of contact which further complicates the analysis. Existing mechanistic approaches including classical plate bending, layered elastic theories, and FEM can not properly describe the conditions in the proximity of tires for near-surface crack initiation. The micromechanical theories employed in discrete element types of methods can be useful; however, they are not computationally efficient in solving large scale problems. In addition, the acquisitions of continuum mechanics theories over the years and adaptability to finite element types of methods are irrevocable. Therefore, a robust and accurate mechanical interpretation of this problem is

required not only to improve understanding of the mechanisms but also to identify the major contributing factors to this failure type.

The analysis of near surface cracking under a dual tire configuration on a relatively thick pavement structure is discussed in this chapter. The GFEM was utilized as the numerical tool to find critical locations for crack initiation in a 3-D mesh. The pavement structure was assumed to have existing defects at the aggregate scale. These defects were in the form of half-penny and circular cracks inserted at different locations and orientations on and near the surface. These cracks, in a scale nearly less than 1% of the global scale of the problem domain, were defined as an independent entity and arbitrarily inserted in the mesh. Critical fracture parameters such as stress intensity factors (K_I and K_{II}) and energy release rate were computed to predict crack initiation. Linear elastic fracture mechanics theories in conjunction with elastic material properties were employed to find critical location and orientation. The extension of the proposed approach to viscoelasticity and a viscoelastic crack model is also presented.

4.2 The Analysis of Near-Surface Cracking in Flexible Pavements

The main focus of the analysis is two folds. The first step was to identify the influence of contact stresses on crack initiation on or near the surface of a typical flexible pavement structure with a relatively thick pavement layer. The most critical location/plane or modes of damage for crack initiation for the given structure and loading can be anticipated using the outcome of the elastic analysis. Secondly, the analysis for one of the most critical cases was extended to viscoelasticity to identify the effects of time and temperature. The analysis was performed by inserting cracks one at a time at various locations in the vicinity of the dual-tires to find the most critical location and orientation for crack initiation and propagation. The results from the analysis are then discussed in light of various crack front parameters.

4.2.1 **Three-Dimensional Pavement Model**

A large scale 3-D model of a flexible pavement structure was developed. Traffic loads were represented by a dual-tire configuration with non-uniform contact stresses as

shown in Figure 4.1. The contact stresses were obtained from earlier studies by the research group (Elseifi et al., 2005, 2006, Yoo and Al-Qadi, 2007, 2008, Al-Qadi et al., 2008, Wang and Al-Qadi, 2009). Thickness of the HMA, base, and subgrade layers were 254, 700, 500 mm, respectively. Half-penny and circular-shaped cracks at aggregate scale were inserted at various locations within the pavement. These cracks have a radius of 5mm. Figure 4.2 illustrates the coordinates of each crack inserted in the mesh with respect to the dual-tire on the surface. The problem was analyzed one crack at a time. The cracks were located at four positions on the surface away from the edge of the dual tires and five depths within the pavement. The cracks were rotated clockwise 30° and 60° to find the most critical plane of cracking. In all, 60 cracks were analyzed in this study.

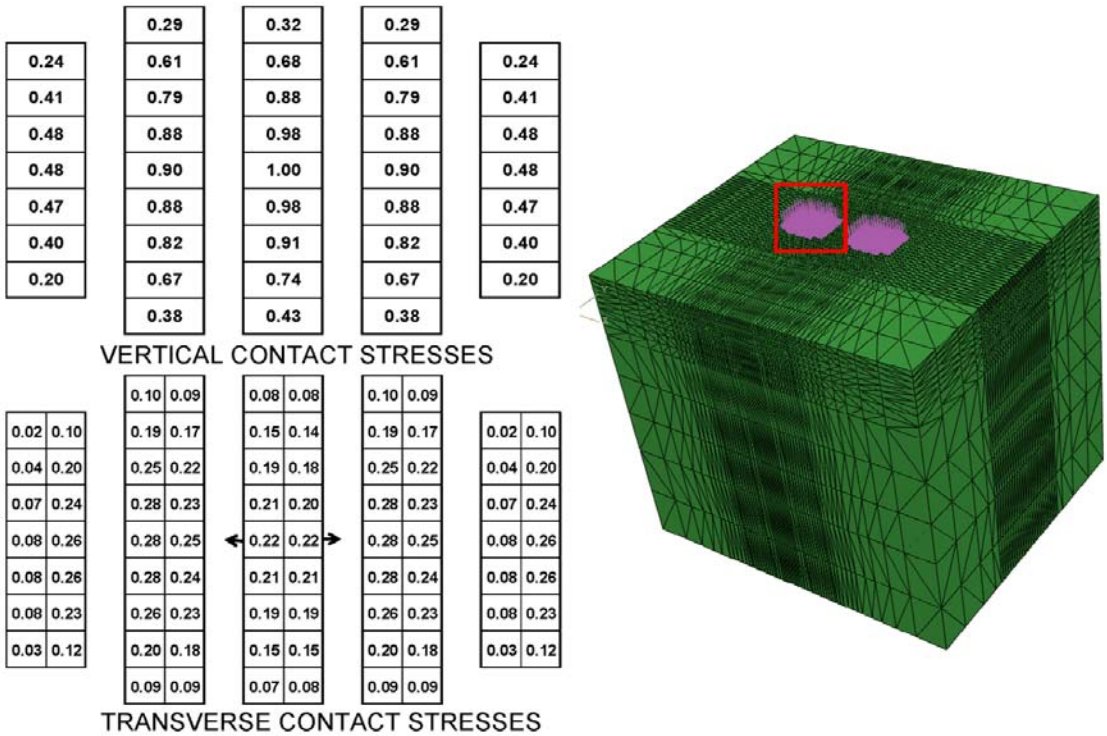

Figure 4.1. Three dimensional pavement model with dual-tire contact stresses on the surface. Normalized transverse and vertical stresses are shown on each rib (contact stresses at each cell of the rib are normalized by the maximum vertical pressure).

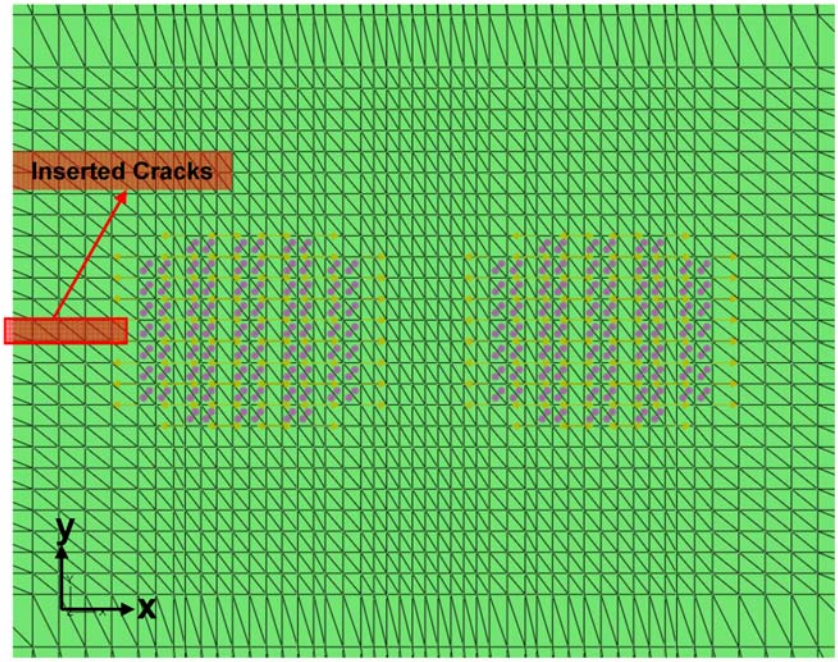

(a)

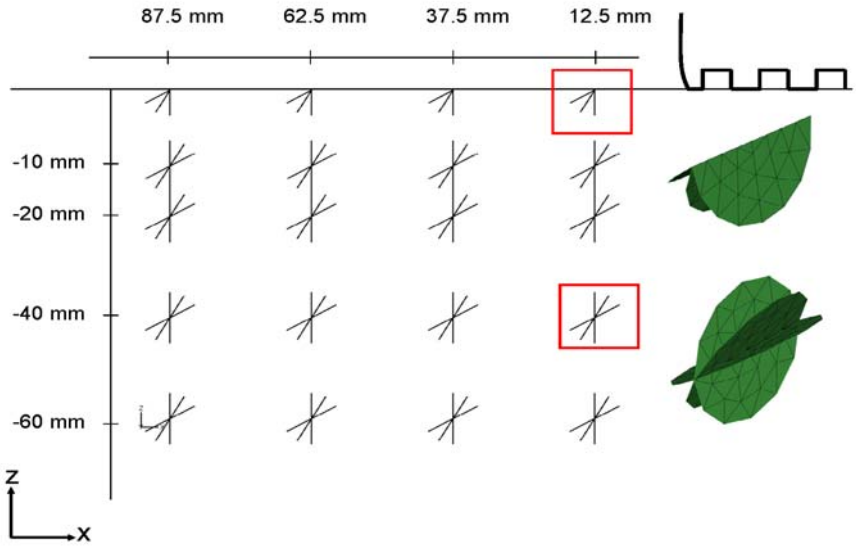

(b)

Figure 4.2. The coordinates of surface and embedded cracks with respect to the dual-tire contact stresses on the pavement surface: (a) Top view of the pavement surface in the

vicinity of dual-tire imprints; and (b) Coordinates of each crack on the surface and within the pavement.

The cracks in the GFEM are a separate entity and modeled with 2-D triangular elements on the plane and 1-D bar elements along the crack front. These elements are not computational elements, which contribute to the stiffness matrix or internal force vector calculations. It is important to note such a depth of analysis is only feasible because cracks are independent of the global coarse mesh, and only one pavement model (without cracks) is generated.

The solution strategy of the fracture problems in the GFEM involves the following basic steps:

- Automatic crack front refinement;
- Automatic assignment of enrichment functions (polynomial, step, and singular) to the selected nodes. The order of approximation (linear, quadratic or cubic) is also chosen at this step;
- Solution of the problem;
- Post-processing the results to compute crack front parameters such as SIF's and *J*-integral.

Crack front refinement is essential in fracture problems. With the automatic refinement applied at the crack fronts, locally graded meshes are generated. Figure 4.3 illustrates locally refined crack fronts from the two analysis cases. The level of refinement and the order of approximation dictate the accuracy of the solution variables (displacements, stresses, strains etc.) at the crack tip. The final size of the elements at the crack front after refinement is in the range between 0.3-0.6mm.

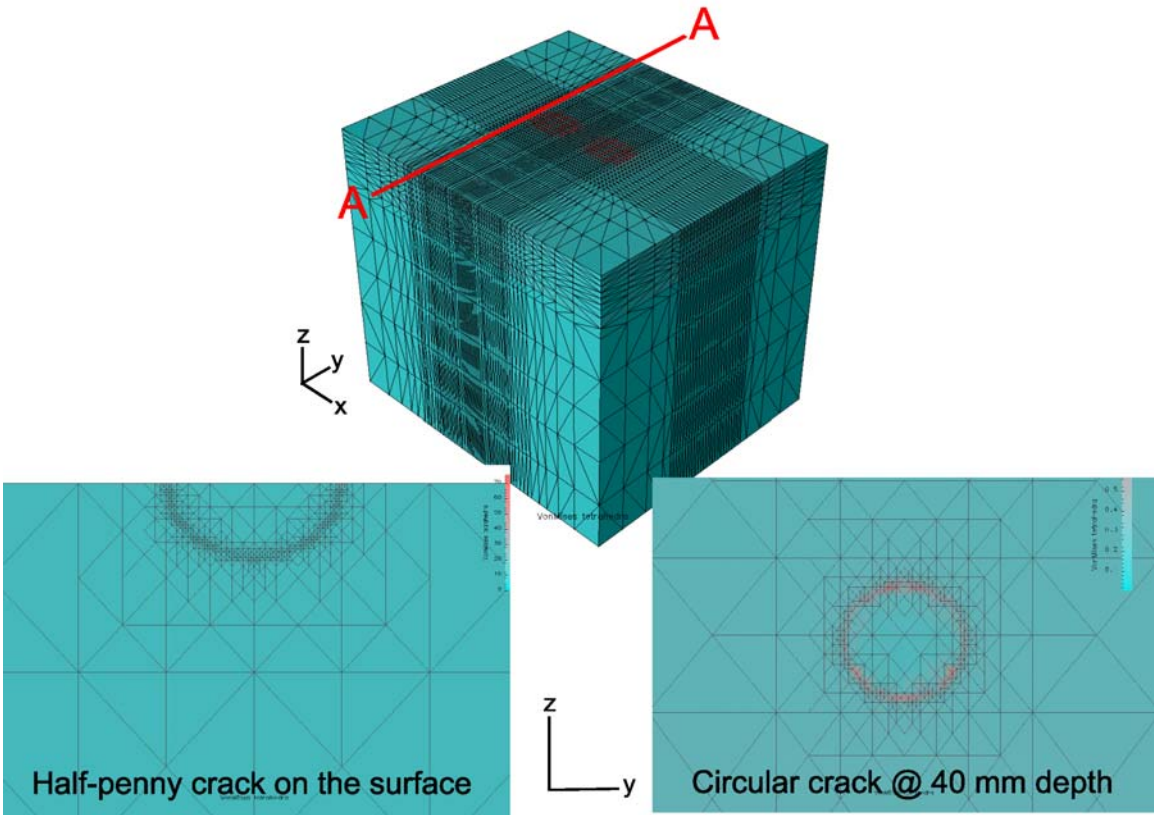

Figure 4.3. Automatic crack front refinement illustrating locally graded meshes at the front domain of half-penny and circular crack.

4.2.2 **Results from the Elastic Solution**

The first step of analysis was conducted using elastic material properties and linear elastic fracture mechanics theories. The purpose of this analysis was to assess the stress states and identify critical modes and locations of cracking in the proximity of dual tires. Elastic modulus and Poisson's ratio of bituminous layer were 17,600 MPa and 0.3, respectively. Base layer modulus and Poisson's ratio were taken 450 MPa and 0.35 whereas subgrade modulus and Poisson's ratio were 150 MPa and 0.35, respectively.

First, multi-axial state of stresses in the vicinity of the tires was assessed using Mohr circle analysis. This part of the analysis was performed without the cracks. Mohr circle representation of the stresses or strains with the use of principal stresses has commonly been used to predict critical planes of damage (Fatemi and Socie, 1988, Socie, 1993). Stresses at various locations under the dual-tire were mapped to the Mohr circles.

Figure 4.4 illustrates the Mohr circles plotted at 4 different locations. The Mohr circle right beneath the dual tires exhibits strong influence of compressive stresses induced by the tire vertical pressure on the surface. The effects of compression diminish away from the tires within the pavement. This was observed at locations denoted by labels 3 and 4, farther away from the tire edge.

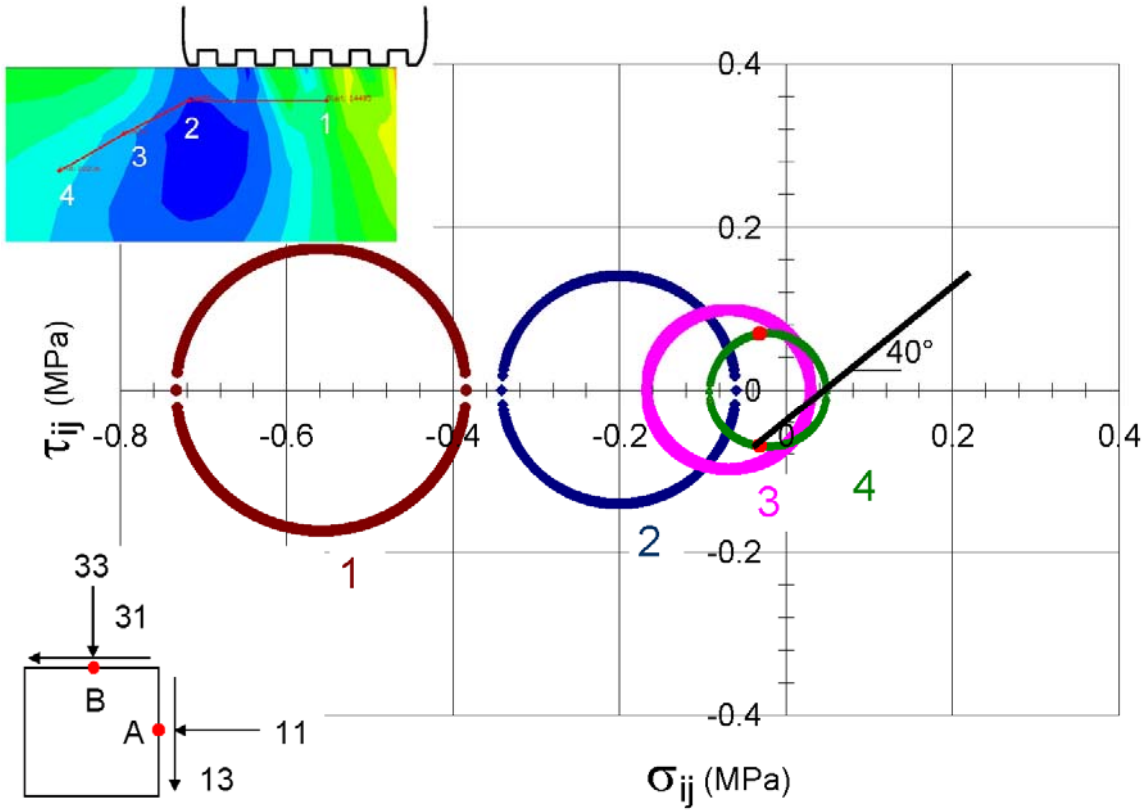

Figure 4.4. Mohr-circle analysis of near-surface stresses under a dual-tire configuration.

The stress states in the proximity of dual-tires indicate the potential for tensile and shear damage. Shear damage is likely in the areas closer to the tire whereas tensile damage can occur in the areas farther away from the tire. Critical planes can then also be identified based on the dominant damage mode. For example, crack growth due to tensile damage will occur on a plane perpendicular to the maximum principal stress according to several models discussed by Fatemi and Socie (1988), Socie (1993). This corresponds to one of the cases shown in Figure 4.4 denoted by 3 and 4. Stress states in these locations

suggest that tensile damage is likely to occur on planes approximately 40° from the horizontal plane. This is the plane on which maximum tensile stresses occur. In all other cases, shear damage is likely to occur on planes where maximum shear stress develops. In this case, damage or crack growth can also be delayed due to presence of mean compressive stresses. It is very important to assess stress conditions appropriately before any fatigue damage or crack growth model can be used. Once the failure mode has been identified, an appropriate fatigue model can be chosen to estimate the service life. Therefore, it is essential to identify the stress conditions for the near-surface cracking problem and find critical planes for crack growth.

In order to find the critical planes for crack growth, each of the cracks presented in the previous section in Figure 4.2 were analyzed one by one. Crack front parameters such as stress intensity factors (SIF's) were computed along the crack fronts. Each location chosen for analysis contains 3 cracks on vertical plane as well as on 30° and 60° rotated planes. The SIF's generally appear to be a smoothly varying function along the crack front. The results from this analysis will be discussed next.

Surface cracks are located at four different locations on the surface as shown in Figure 4.2.These are all half-penny shaped cracks on vertical, 30° and 60° rotated planes. Figure 4.5 illustrates the results from these cracks. Mode-I and mode-II SIF's are shown along the front of each crack. Crack front parameters were computed along the crack front of a 2-D curved crack surface except the edge vertices that meet the boundary of the problem domain.

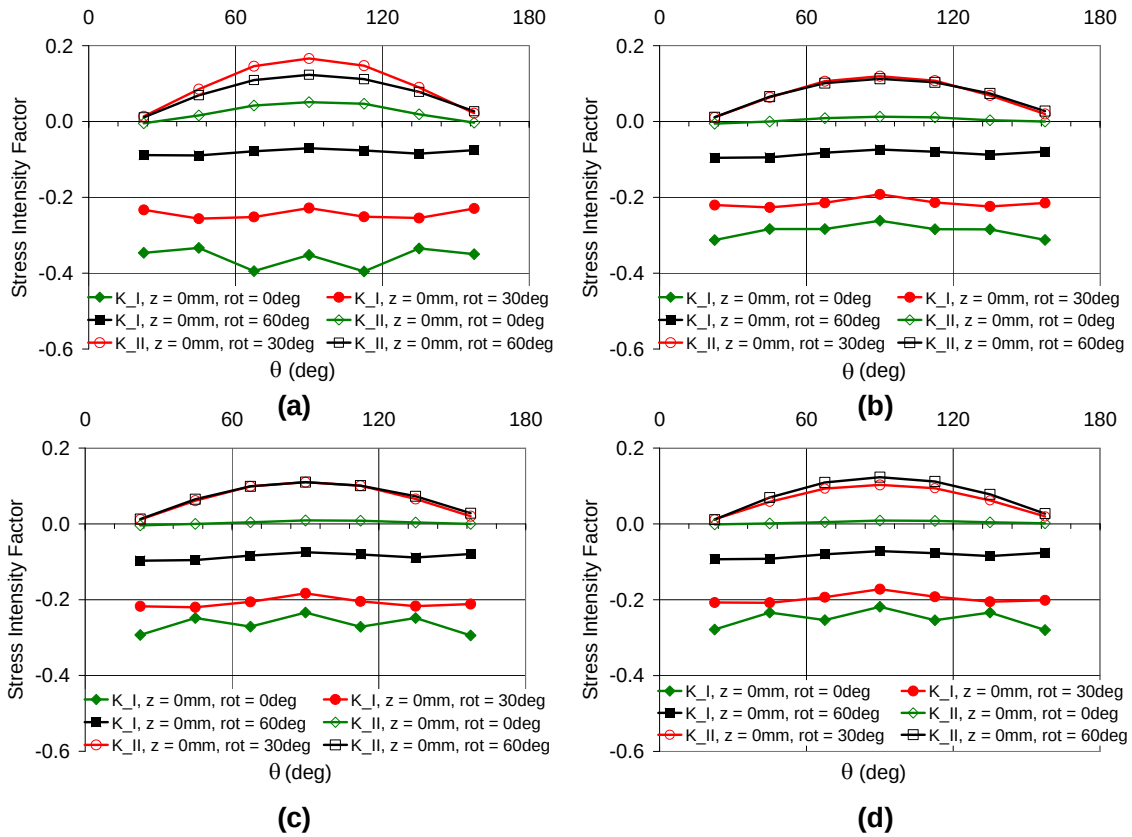

Figure 4.5. Stress intensity factors (K_I and K_{II}) computed along the curved crack front (from θ=0° to 180°) of half-penny shaped cracks on the surface: (a) Cracks at 12.5 mm away from the tire edge; (b) Cracks at 37.5 mm away from the tire edge; (c) Cracks at 62.5 mm away from the tire edge; and (d) Cracks at 87.5 mm away from the tire edge.

Strong influence of compression is apparent at all crack planes and all positions. The influence of mode-II fracture is noticeable; however, the degree of mode-II fracture increases on the rotated planes. Based on the results of obtained cracks at four different locations, it was concluded that there is no likelihood of tensile damage on the surface at these locations. Shear damage could become an issue, however. But the presence of compression will certainly delay the initiation and propagation of cracks.

Similar to the case of surface cracks, circular cracks were inserted at four different locations within the pavement. The coordinates of each of these cracks are shown in

Figure 4.2. Circular cracks were located at four different depths (10, 20, 40, and 60 mm within the pavement). The results from all depths are presented herein.

Figure 4.6 shows the stress intensity factors computed along the fronts of cracks at 10 mm deep in the pavement. Similar to the surface cracks, a strong compression effect is evident at the crack fronts. The magnitude of compression which is inferred by the K_I values decreases on the rotated planes. It nearly diminishes to 0 on the plane of 60°. Further from the tire edge, the influence of compression along the crack fronts begins to vanish.

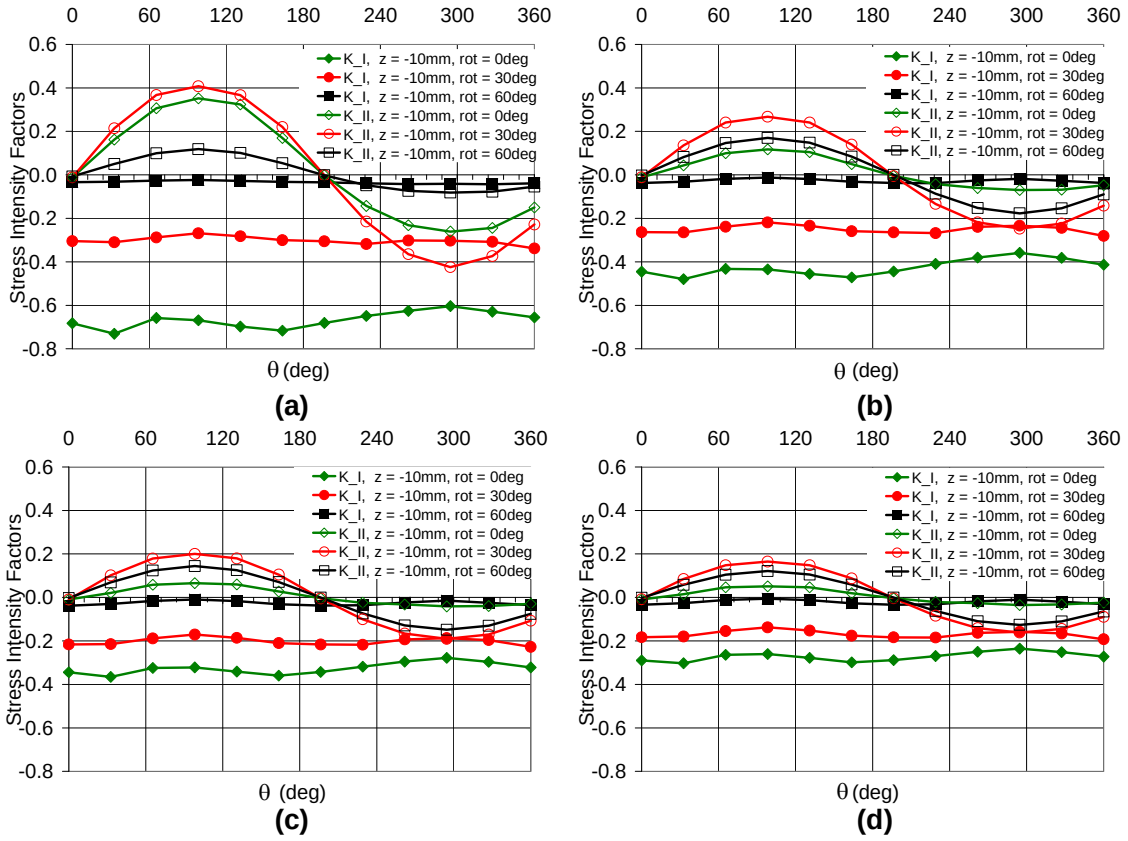

Figure 4.6. Stress intensity factors (K_I and K_{II}) computed along the curved crack front (from θ=0° to 360°) of circular shaped cracks at 10 mm depth: (a) Cracks at 12.5 mm away from the tire edge; (b) Cracks at 37.5 mm away from the tire edge; (c) Cracks at 62.5 mm away from the tire edge; and (d) Cracks at 87.5 mm away from the tire edge.

The effect of mode-II fracture is also evident from K_{II} values at all cracks. The magnitude of K_{II} is more pronounced on the vertical planes. As the rotation angle increases, the magnitude of K_{II} decreases. However, the effect of mode-II remains significant regardless of the crack location and orientation. The analysis at this depth shows the significance of shear stresses that becomes the main cause of crack growth at this location.

Figures 4.7 to 4.9 show similar results from the cracks at 20, 40, and 60mm depths. As the depth of crack increases, the crack front states also change slightly. The effects of compression diminish and some cracks start exhibiting a tensile mode of fracture. This is illustrated by the K_I values particularly on the 60° crack planes at 60 mm depth. The position, where maximum positive K_I is attained (crack at 87.5 mm away from tire edge and on 60° plane as shown in Figure 4.9, can be considered the most critical location for crack growth in tension mode. This observation is also in agreement with the work done earlier to investigate top-down cracking in thick flexible pavements (Yoo and Al-Qadi, 2007, 2008).

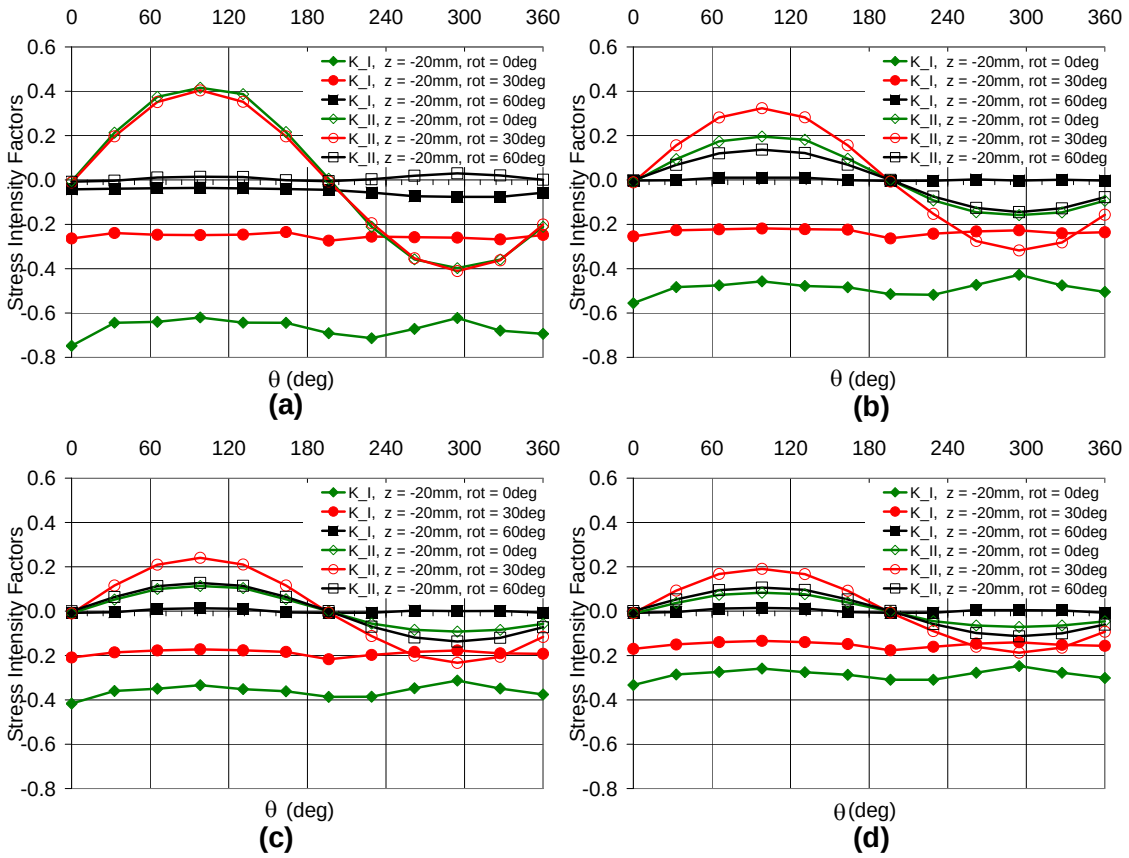

Figure 4.7. Stress intensity factors (K_I and K_{II}) computed along the curved crack front (from θ=0° to 360°) of circular shaped cracks at 20 mm depth: (a) Cracks at 12.5 mm away from the tire edge; (b) Cracks at 37.5 mm away from the tire edge; (c) Cracks at 62.5 mm away from the tire edge; and (d) Cracks at 87.5 mm away from the tire edge.

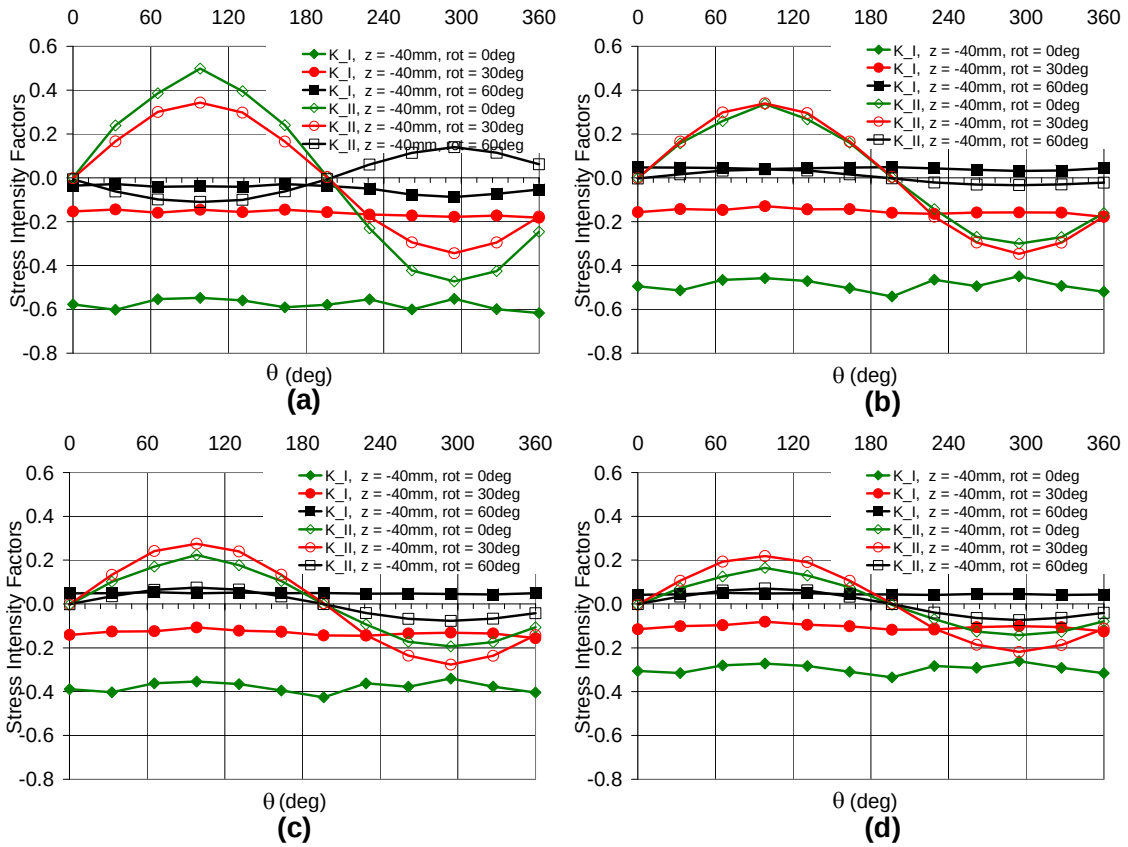

Figure 4.8. Stress intensity factors (K_I and K_{II}) computed along the curved crack front (from θ=0° to 360°) of circular shaped cracks at 40 mm depth: (a) Cracks at 12.5 mm away from the tire edge; (b) Cracks at 37.5 mm away from the tire edge; (c) Cracks at 62.5 mm away from the tire edge; and (d) Cracks at 87.5 mm away from the tire edge.

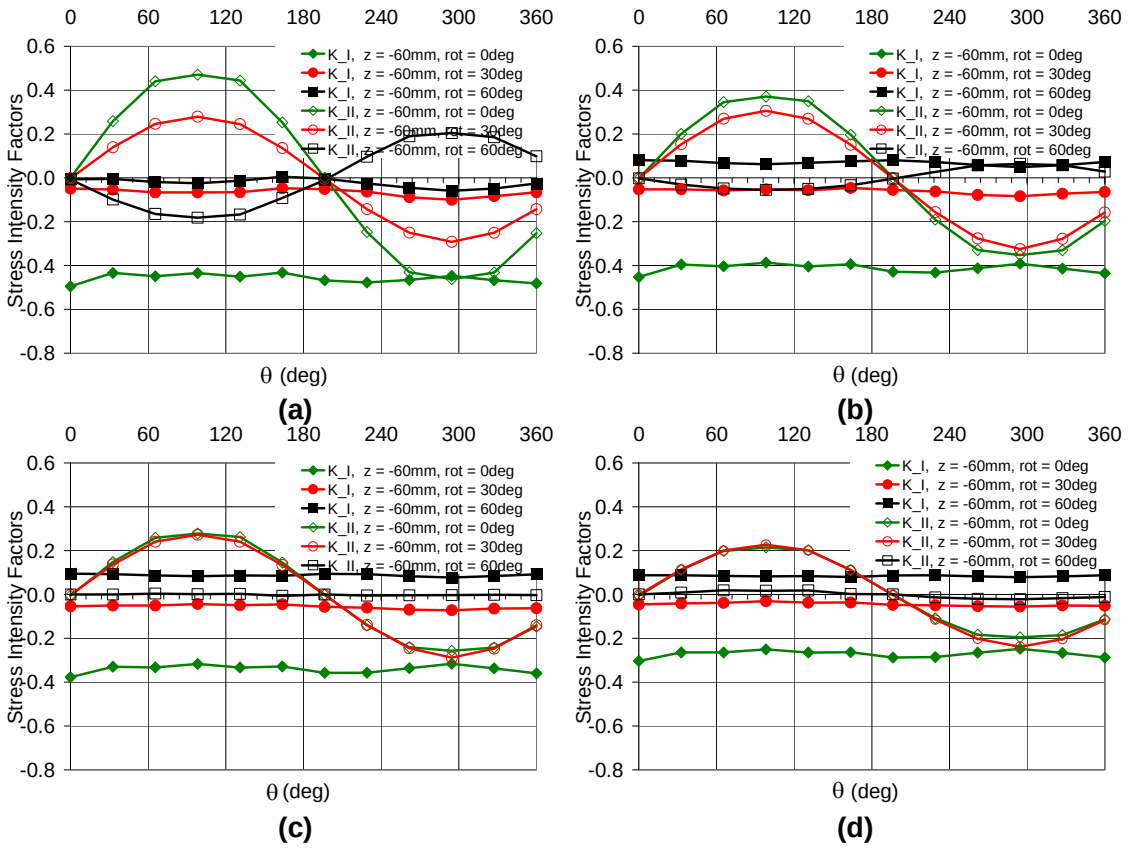

Figure 4.9. Stress intensity factors (K_I and K_{II}) computed along the curved crack front (from θ=0° to 360°) of circular shaped cracks at 60 mm depth: (a) Cracks at 12.5 mm away from the tire edge; (b) Cracks at 37.5 mm away from the tire edge; (c) Cracks at 62.5 mm away from the tire edge; and (d) Cracks at 87.5 mm away from the tire edge.

4.2.3 **Viscoelastic Crack Analysis**

Elastic crack analysis demonstrates the critical modes of near-surface damage due to a dual-tire configuration. A viscoelastic analysis was also performed at one of the critical locations to capture time-dependent response of the bulk material as well as crack front zone. The Generalized Maxwell Model was used as a mechanical analog to represent relaxation characteristics of viscoelastic materials and integrated to a nonlinear Newton-Raphson iterative scheme.

The domain integral approach and Schapery's viscoelastic crack model was used to compute energy release rate along the front of the most critical crack case. Details of domain integral to compute *J*-integral and Schapery's work of fracture method for viscoelastic materials was discussed in the preceding chapters in details. Viscoelastic analysis was performed for one of the most critical cases presented with elastic analysis of the same problem. The analyzed case had a crack at 60 mm depth and rotated to a 60. plane. As shown with the SIF's in Figure 4.9 (the crack 87.5 mm away from the tire edge), the tension mode of failure dominates in this case along the crack front. Figure 4.10 illustrates the viscoelastic material properties used in the solution of the problem and as well as in the computation of the work of fracture. The master curve for this material was obtained using complex modulus tests conducted at five temperatures spanning -10 to 54°C and frequencies 0.1 to 25 Hz.

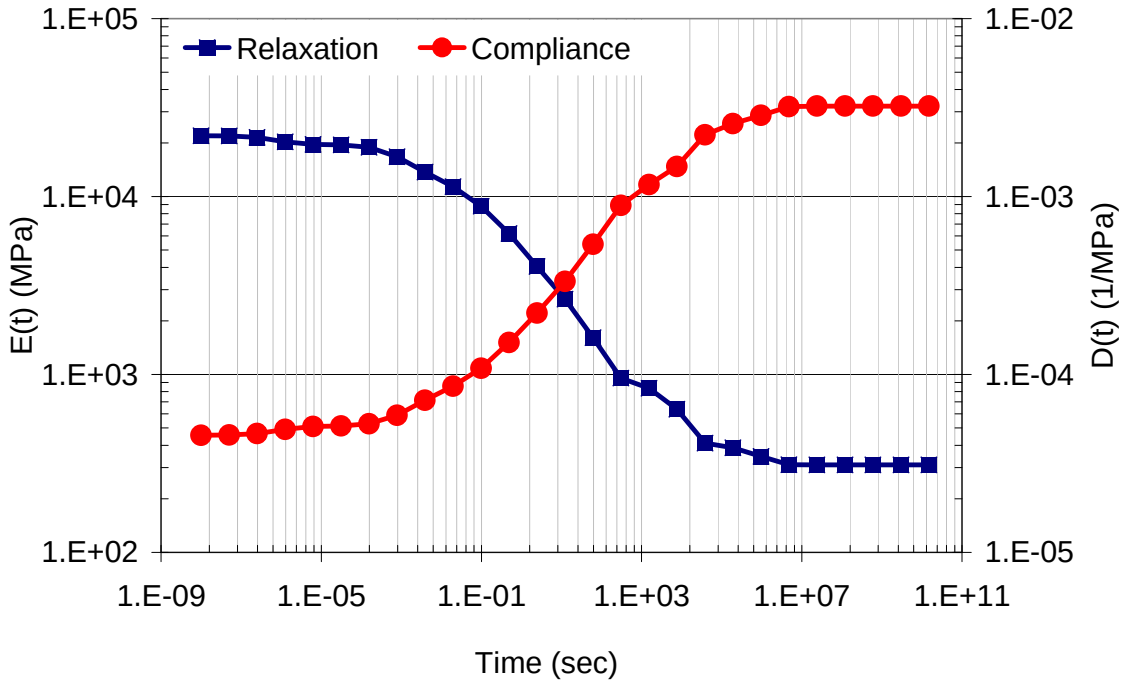

Figure 4.10. Prony series representation of the relaxation and compliance functions. where E_m and D_m are the relaxation and compliance coefficients of Prony series.

The same dual-tire contact stresses were applied on the surface of the pavement. Load variation with time was described with a half-sinusoidal amplitude-time curve. The duration of pulse was used as 0.03 seconds simulating loading times obtained from moving truck at average speeds as well as from FWD testing (Loulizi et al., 2002). The analysis was performed at various temperatures to illustrate the effect of temperature on the work of fracture.

Figure 4.11 demonstrates the variation of the work of fracture and the generalized *J*-integral (J_v) with time from the analysis at −10°C and 21°C. By definition, the generalized *J*-integral describes the energy available for crack growth in a corresponding elastic state, which does not consider time and temperature effects. On the other hand, the work of fracture represents the time and temperature dependent nature of the crack front damage zone. As shown in this figure with the results at 21°C, the work of fracture departs from the J_v illustrating an amplification in the available energy due to viscoelastic effects at the crack front. The difference between work of fracture and J_v diminishes for the case analyzed at −10°C, which implies negligible viscoelastic effects at low temperatures.

Energy release rate is one of the most significant crack tip parameters that can be used for computing the magnitude of crack growth for inelastic materials such as plastic or viscoelastic materials. Accurate computation of energy release rate with consideration of temperature and rate effects is essential for the near-surface failure characterization of pavements. Schapery's generalized *J*-integral approach for viscoelastic materials offers a practical methodology when it is combined with the domain integral theories derived for 3-D fracture mechanics problems. The numerical approach proposed in this study, on the hand, allows the understanding of the near-surface cracking mechanisms considering 3-D effects of tire-pavement interaction as well as the effect of material viscoelasticity.

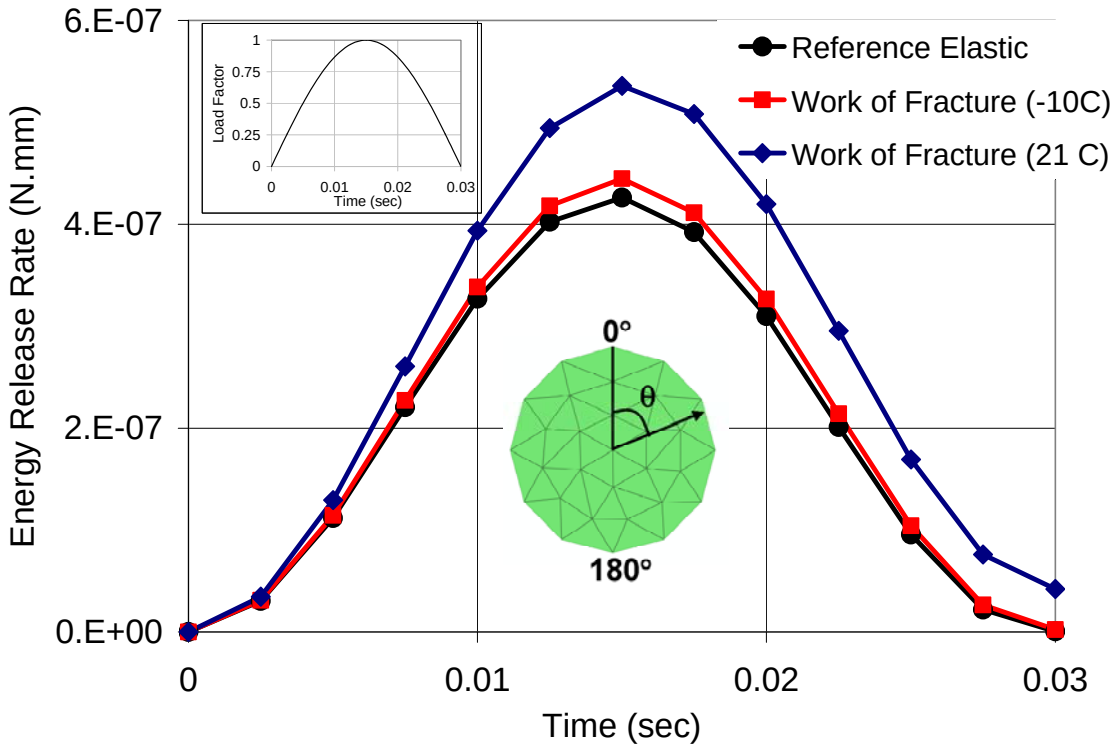

Figure 4.11. The energy release rate computed at θ=90° along the circular crack at 60 mm depth and 60° plane to illustrate viscoelastic effects at −10°C and 21°C.

4.3 Summary and Remarks

A novel computational methodology was used to analyze the near-surface cracking problem in thick asphalt pavements. The analysis identified the extent of the effects of the tire contact stresses on developing near-surface cracking potential. The GFEM is a very promising computational tool for 3-D fracture problems because it eliminates crack front meshing problems and increases the accuracy of the solution at the crack fronts. This numerical tool was utilized to characterize near-surface cracking in flexible pavements. Sixty different cases, each containing one crack at a different location or orientation, were analyzed efficiently owing to the computational structure of the GFEM. A single user generated mesh was used in all cases. In contrast, such analysis with the standard FEM would require a user generated mesh for each one of the cases

considered which would render the analysis quite difficult and extremely time consuming.

The analysis of the cracks in the proximity of the dual-tires showed strong mixed-mode fracture conditions almost everywhere near the surface. Shear mode of fracture in the presence of compression appears to be the dominant mode of damage. However, tensile mode of fracture also starts to emerge on 30−60° rotated planes and approximately at 60 mm depth from the surface, which is also in agreement with the work done earlier (Yoo and Al-Qadi, 2007, 2008). Elastic analysis was carried out to identify the critical mode of fracture and locations. The stress states and strong influence of mode mixity will not likely be altered with consideration of viscoelasticity in such a problem where load boundary conditions were applied. Therefore, the discussions and outcome presented in this study can shed light on the experimental characterization of the near-surface cracking phenomenon which appears to be driven by very different stress conditions than the classical fatigue cracking approach. This study also highlights the impact novel computational methods like the GFEM can have on the discovery and understanding the mechanisms governing the premature failure of pavements.

The same large scale pavement problem was also extended to viscoelasticity to identify the effects of creep on crack front parameters. Since the SIF's cannot be computed for inelastic materials, crack front conditions were characterized by energy release rate in the form of the *J*-integral. Schapery's generalized *J*-integral approach was extended to domain integral form to analyze 3-D fracture problems considering viscoelastic material properties. The *J*-integral with the form presented and used in this study captures 3-D effects emanating from the tire contact stresses, especially very influential near the surface of pavements, as well as viscoelastic effects. This form of *J*-integral in conjunction with the GFEM can be used as a tool in a pavement design protocols to compute the increment of crack growth that might occur on or near the surface of pavements; hence to predict failure time of pavements more accurately.

CHAPTER 5. CONCLUSIONS

This chapter summarizes the research, highlights its contributions, and proposes directions for future research.

5.1 Summary

A novel computational methodology was used to analyze the near-surface cracking problem in thick asphalt pavements. The analysis identified the extent of the effects of the tire contact stresses on developing near-surface cracking potential. The GFEM is a very promising computational tool for 3-D fracture problems because it eliminates crack front meshing problems and increases the accuracy of the solution at the crack fronts. This numerical tool was utilized to characterize near-surface cracking in flexible pavements. Sixty different cases, each containing one crack at a different location or orientation, were analyzed efficiently owing to the computational structure of the GFEM. A single user generated mesh was used in all cases. In contrast, such analysis with the standard FEM would require a user generated mesh for each one of the cases considered which would render the analysis quite difficult and extremely time consuming.

The analysis of the cracks in the proximity of the dual-tires showed strong mixed-mode fracture conditions almost everywhere near the surface. Shear mode of fracture in the presence of compression appears to be the dominant mode of damage. However, tensile mode of fracture also starts to emerge on 30-60° rotated planes and approximately at 60mm depth from the surface, which is also in agreement with the work done earlier

(Yoo and Al-Qadi, 2007, 2008). Elastic analysis was carried out to identify the critical mode of fracture and locations. The stress states and strong influence of mode mixity will not likely be altered with consideration of viscoelasticity in such a problem where load boundary conditions are applied. Therefore, the discussions and outcome presented in this study can shed light on the experimental characterization of the near-surface cracking phenomenon which appears to be driven by very different stress conditions than the classical fatigue cracking approach. This study also highlights the impact novel computational methods like the GFEM can have on the discovery and understanding of mechanisms governing the premature failure of pavements.

The same large scale pavement problem was also extended to viscoelasticity to identify the effects of creep on crack front parameters. Since the SIF's can not be computed for inelastic materials, crack front conditions are characterized by energy release rate in the form of the *J*-integral. Schapery's generalized *J*-integral approach was extended to domain integral form to analyze 3-D fracture problems considering viscoelastic material properties. The *J*-integral with the form presented and used in this study captures 3-D effects emanating from the tire contact stresses, especially very influential near the surface of pavements, as well as viscoelastic effects. This form of *J*-integral in conjunction with the GFEM can be used as a tool in a pavement design protocols to compute the increment of crack growth that might occur on or near the surface of pavements; hence to predict failure time of pavements more accurately.

5.2 Future research directions

The present research addressed the problem of near surface cracking in thick flexible pavements. It is proposed that the present research can be solved using a novel numerical methodology recently emerged for the solution of fracture problems. Experimental and field validation of the numerical models utilized is required. In addition, numerical methodology should be adapted to consider the effects of moving load and other nonlinear material behavior.

REFERENCES

Alfano, G. and Crisfield, M.A. (2001). Finite element interface models for the delamination analysis of laminated composites: mechanical and computational issues. International Journal for Numerical Methods in Engineering, 50(7):1701–1736.

Alfano, G. and Crisfield, M.A. (2003). Solution strategies for the delamination analysis based on a combination of local-control arc-length and line searches. International Journal for Numerical Methods in Engineering, 58(7):999–1048.

Alfano, G. and Sacco, E. (2006). Combining interface damage and friction in a cohesive-zone model. International Journal for Numerical Methods in Engineering, 68(5):542–582.

Al-Qadi, I. L., Wang H., Yoo, P. J., and Dessouky, S. H. (2008). Dynamic Analysis and In-Situ Validation of Perpetual Pavement Response to Vehicular Loading. In Transportation Research Record: Journal of the Transportation Research Board, No. 2087, Transportation Research Board of the National Academies, Washington D.C., pp. 29–39.

Carol, I., Lopez, C. M., and Roa, O. (2001). Micromechanical analysis of quasi-brittle materials using fracture-based interface elements. International Journal for Numerical Methods in Engineering, 52(1-2):193–215.

Chaboche, J. L., Girard R., and Levasseur, P. (1997a). On the interface debonding models. International Journal of Damage Mechanics, 6(3):220.

Chaboche J. L., Girard R., and Schaff A. (1997b). Numerical analysis of composite systems by using interphase/interface models. Computational Mechanics, 20(1):3–11.

De Freitas, E. F., Pereira, P., Santos, L. P., and Papagiannakis, A.T. (2005). Effect of Construction Quality, Temperature, and Rutting on Initiation of Top-Down Cracking. In Transportation Research Record: Journal of the Transportation Research Board, No. 1929, Transportation Research Board of the National Academies, Washington D.C., pp. 174–182.

Desai C.S., Zaman, M. M., Lightner, J.G., and Siriwardane, H.J. (1984). Thin-layer element for interfaces and joints. International Journal for Numerical and Analytical Methods in Geomechanics, 8(1):19–43.

Desai, C. S., Drumm, E.C., and Zaman, M. M. (1985). Cyclic testing and modeling of interfaces. Journal of Geotechnical Engineering, 111:793.

Dolbow, J., Moes, N. and Belytschko, T. (2000). Discontinuous enrichment in finite elements with a partition of unity method. Finite Elements in Analysis & Design, 36(3-4):235–260.

Duarte, C. A., Hamzeh, O. N., Liszka, T.J. and Tworzydlo, W.W. (2001). A generalized finite element method for the simulation of three-dimensional dynamic crack propagation. Computer Methods in Applied Mechanics and Engineering, 190(15-17):2227–2262.

Duarte, C. A. Babuska, I. and Oden, J. T. (2000). Generalized finite element methods for three-dimensional structural mechanics problems. Computers and Structures, 77(2):215–232.

Duarte, C. A. and Oden, J. T. (1996a). An hp adaptive method using clouds. Computer Methods in Applied Mechanics and Engineering, 139(1-4):237–262.

Duarte, C. A. and Oden, J. T. (1996b). Hp clouds-an hp meshless method. Numerical Methods for Partial Differential Equations, 12(6):673–706.

Elseifi, M., Al-Qadi, I. L., and Yoo, P. J. (2006). Viscoelastic Modeling and Field Validation of Flexible Pavements. In Journal of Engineering Mechanics, vol. 132, 2006, pp. 172-178.

Elseifi, M., Al-Qadi, I. L., Yoo, P. J., and Janajreh, I. (2005). Quantification of Pavement Damage Caused by Dual and Wide-Base Tires. In Transportation Research Record: Journal of the Transportation Research Board, No. 1940, Transportation Research Board of the National Academies, Washington D.C., pp. 125–135.

Fatemi, A. and Socie, D. F. (1988). A critical plane approach to multiaxial fatigue damage including out-of-phase loading. Fatigue & Fracture of Engineering Materials & Structures, 11(3):149–165.

Kim, J., Roque, R., and Byron, T. (2009). Viscoelastic analysis of flexible pavements and its effects on top-down cracking. In Journal of Materials in Civil Engineering, pp. 324-332.

Kim, D. J., Duarte, C. A. and Pereira, J. P. (2008). Analysis of interacting cracks using the generalized finite element method with global-local enrichment functions. Journal of Applied Mechanics, 75:051107.

Kim, D. J., Pereira, J. P., and Duarte, C.A. (2009). Analysis of three-dimensional fracture mechanics problems: A two-scale approach using coarse-generalized FEM meshes. International Journal for Numerical Methods in Engineering, 81(3):335–365.

Knauss, W. G. (1989) Time dependent fracture of polymers. Advances in Fracture Research, 4:2683–2711.

Li, S., Mear, M. E. and Xiao, L. (1998). Symmetric weak-form integral equation method for three-dimensional fracture analysis. Computer methods in applied mechanics and engineering, 151(3-4):435–459.

Loulizi, A. Al-Qadi, I. L., Lahouar, S. and Freeman, T.E. (2002). Measurement of Vertical Compressive Stress Pulse in Flexible Pavements: Representation for Dynamic Loading Tests. Transportation Research Record: Journal of the Transportation Research Board, 1816(-1):125–136.

Mahtab, M., and Goodman, R. E. (1970) Three dimensional analysis of joint rock slope. In Proc. of the 2nd Int. Congress of ISRM, pages 353–360. Belgrade (Yugoslavia).

Masuero, J. R. and Creus, G. J. (1993). Finite elements analysis of viscoelastic fracture. International Journal of Fracture, 60(3):267–282.

Masuero, J. R. and Creus, G. J. (1995). Crack growth initiation in concrete-like materials in the presence of creep. Nuclear Engineering and Design, 156(1):209–218.

Moes, N., Gravouil, A. and Belytschko, T. (2002). Non-planar 3D crack growth by the extended finite element and level sets-Part I: Mechanical model. Int. J. Numer. Meth. Engng, 53:2549–2568.

Moran, B. and Shih, C. F. (1987). Crack tip and associated domain integrals from momentum and energy balance. Engineering Fracture Mechanics, 27(6):615–642.

Myers, L., Roque, R., and Birgisson, G. (2000). Propagation Mechanisms for Surface-Initiated Longitudinal Wheelpath Cracks. In Transportation Research Record: Journal of the Transportation Research Board, No. 1778, Transportation Research Board of the National Academies, Washington D.C., pp. 113–122.

Mueller, H. K. (1971). Stress-intensity factor and crack opening for a linearly viscoelastic strip with a slowly propagating central crack. International Journal of Fracture, 7(2):129–141.

Oden, J. T. and Duarte, C.A. (1997). Clouds, cracks and fems. Recent Developments in Computational and Applied Mechanics, pages 302–321.

Ortiz, M. and Pandolfi, A. (1999). Finite-deformation irreversible cohesive elements for three-dimensional crack-propagation analysis. International Journal for Numerical Methods in Engineering, 44(9):1267–1282.

Pereira, J. P. and Duarte, C.A. (2004). Computation of stress intensity factors for pressurized cracks using the generalized finite element method and superconvergent extraction techniques. In XXV Iberian Latin-American Congress on Computational Methods in Engineering, Recife, PE, Brazil.

Pereira, J. P. and Duarte, C.A. (2005). Extraction of stress intensity factors from generalized finite element solutions. Engineering analysis with boundary elements, 29(4):397–413.

Pereira, J.P. and Duarte, C. A. (2006). The contour integral method for loaded cracks. Communications in Numerical Methods in Engineering, 22(5):421–432, 2006.

Pereira, J. P., Duarte, C. A. Guoy, D. and Jiao, X. (2009a). Hp-Generalized FEM and crack surface representation for non-planar 3-D cracks. International Journal for Numerical Methods in Engineering, 77(5):601–633.

Pereira, J. P., Duarte, C. A. Guoy, D. and Jiao, X. (2009b). Generalized finite element method enrichment functions for curved singularities in 3D fracture mechanics problems. Computational Mechanics, 44(1):73–92.

Pitti, R. M., Dubois, F., Petit, C. and Sauvat, N. (2007). Mixed mode fracture separation in viscoelastic orthotropic media: numerical and analytical approach by the M q v-integral. International Journal of Fracture, 145(3):181–193.

Rice, J. R. (1968). A path independent integral and the approximate analysis of strain concentration by notches and cracks. Journal of applied mechanics, 35(2):379–386.

Rolt, J. (2000). Top-down cracking: myth or reality. The World Bank Regional Seminar on Innovative Road Rehabilitation and Recycling Technologies, Amman, Jordan.

Schapery, R. A. (1975a). A theory of crack initiation and growth in viscoelastic media. International Journal of Fracture, 11(1):141–159.

Schapery, R. A. (1975b). A theory of crack initiation and growth in viscoelastic media II. Approximate methods of analysis. International Journal of Fracture, 11(3):369–388.

Schapery, R. A. (1975c). A theory of crack initiation and growth in viscoelastic media. III- Analysis of continuous growth. International Journal of Fracture, 11:549–562.

Schapery, R. A. (1984). Correspondence principles and a generalized J integral for large deformation and fracture analysis of viscoelastic media. International Journal of Fracture, 25(3):195–223.

Schapery, R. A. (1990). On some path independent integrals and their use in fracture of nonlinear viscoelastic media. International Journal of Fracture, 42(2):189–207.

Shih, C. F., Moran, B. and Nakamura, T. (1986). Energy release rate along a three-dimensional crack front in a thermally stressed body. International Journal of Fracture, 30(2):79–102.

Simone, A., Duarte, C. A. and Van der Giessen, E. (2006). A generalized finite element method for polycrystals with discontinuous grain boundaries. Int. J. Numer. Meth. Engng, 67:1122–1145.

Socie, D. F. (1993). Critical plane approaches for multiaxial fatigue damage assessment. Advances in multiaxial fatigue, pages 7–36.

Soon Lee, S. and Jong Kim, Y. (1995). Time-domain boundary element analysis of cracked linear viscoelastic solids. Engineering Fracture Mechanics, 51(4):585–590.

Stankowski, T. and Runesson, K. (1993). Fracture and slip of interfaces in cementitious composites. I: Characteristics. Journal of Engineering Mechanics, 119:292.

Strouboulis, T., Zhang, L., and Babuska, I. (2004). p-version of the generalized FEM using mesh-based handbooks with applications to multiscale problems. Int. J. Numer. Meth. Engng, 60:1639–1672.

Strouboulis, T., Copps, K. and Babuska, I. (2001). The generalized finite element method. Computer methods in applied mechanics and engineering, 190(32-33):4081–4193.

Sukumar, N., Moes, N. Moran, B. and Belytschko, T. (2000). Extended finite element method for threedimensional crack modelling. Int. J. Numer. Meth. Engng, 48:1549–1570.

Sukumar, N., Chopp, D. L., Moes, N. and Belytschko, T. (2001). Modeling holes and inclusions by level sets in the extended finite element method. Computer methods in applied mechanics and engineering, 190(46-47):6183–6200.

Sukumar, N., Srolovitz, D.J., Baker, T. J. and Prevost, J.H. (2003). Brittle fracture in polycrystalline microstructures with the extended finite element method. Int. J. Numer. Meth. Engng, 56:2015-2037.

Suo, Z., Prevost, J. H. and Liang, J. (2003). Kinetics of crack initiation and growth in organic-containing integrated structures. Journal of the Mechanics and Physics of Solids, 51(11-12):2169–2190.

Svasdisant, T., Schorsch, M., Baladi G., and Pinyosunun, S. (2002). Mechanistic Analysis of Top-Down Cracks in Asphalt Pavements. In Transportation Research Record: Journal of the Transportation Research Board, No. 1809, Transportation Research Board of the National Academies, Washington D.C., pp. 126–136.

Uhlmeyer, J. S., Willoughby, K., Pierce, L. M., and Mahoney, J. P. (2000). Top-Down Cracking in Washington State Asphalt Concrete Wearing Courses. In Transportation Research Record: Journal of the Transportation Research Board, No. 1730, Transportation Research Board of the National Academies, Washington D.C., pp. 110–116.

Wang, L. B., Myers, L. A., Mohammad, L. N., and Fu, Y. R. (2003). Micromechanics Study on Top-Down Cracking. In Transportation Research Record: Journal of the Transportation Research Board, No. 1853, Transportation Research Board of the National Academies, Washington D.C., pp. 121–133.

Wang, J., Birgisson, B., and Roque, R. (2007). Windows-Based Top-Down Cracking Design Tool for Florida: Using Energy Ratio Concept. In Transportation Research Record: Journal of the Transportation Research Board, No. 2037, Transportation Research Board of the National Academies, Washington D.C., pp. 86–96.

Wang, H. and Al-Qadi, I. L. (2009). Combined Effect of Moving Wheel Loading and Three-Dimensional Contact Stresses on Perpetual Pavement Responses. In Transportation Research Record: Journal of the Transportation Research Board, No. 2095 Transportation Research Board of the National Academies, Washington D.C., pp. 53–61.

Xu, X. P. and Needleman, A. (1994). Numerical simulations of fast crack growth in brittle solids. Journal of the Mechanics and Physics of Solids, 42(9):1397–1434.

Yoo, P. J. and Al-Qadi, I. L. (2007). Effect of Transient Dynamic Loading on Flexible Pavements. In Transportation Research Record: Journal of the Transportation Research Board, No. 1990, Transportation Research Board of the National Academies, Washington D.C., pp. 129–140.

Yoo, P. J. and Al-Qadi, I. L. (2008). The Truth and Myth of Fatigue Cracking Potential in Hot-Mix Asphalt: Numerical Analysis and Validation. In Journal of the Association of Asphalt Paving Technologists, Vol. 77, pp. 549–590.

Zienkiewicz, C., Best B., Dullage, C., and Stagg, K.G. (1970). Analysis of nonlinear problems in rock mechanics with particular reference to jointed rock systems. Proceedings of International Society of Rock Mechanics.